THE ENHANCEMENT OF COMPOSITE PHASE CHANGE MATERIAL TOWARDS THERMO-PHYSICAL PROPERTIES USING NANOPARTICLE FOR THERMAL ENERGY STORAGE

MUHAMMAD BAKRI BIN AHMAD

UNIVERSITI TEKNIKAL MALAYSIA MELAKA

THE ENHANCEMENT OF COMPOSITE PHASE CHANGE MATERIAL TOWARDS THERMO-PHYSICAL PROPERTIES USING NANOPARTICLE FOR THERMAL ENERGY STORAGE

MUHAMMAD BAKRI BIN AHMAD

A report submitted

in fulfillment of the requirements for the degree of

Bachelor of Mechanical Engineering

Faculty of Mechanical Engineering

UNIVERSITI TEKNIKAL MALAYSIA MELAKA

2020

DECLARATION

I declare that this project report entitled "The Enhancement of Composite Phase Change Material Towards Thermo-Physical Properties using Nanoparticle for Thermal Energy Storage" is the result of my own work except as cited in the references

Signature : .....

Name : .....

Date : .....

APPROVAL

I hereby declare that I have read this project report and in my opinion this report is enough in terms of scope and quality for the award of Bachelor of Mechanical Engineering with Honours.

Signature : .....

Supervisor's Name : .....

Date : .....

DEDICATION

I dedicated this project to all those respectful beings who have helped me in any way to become what I am today. Whose sacrifices seeded our success especially our parents who have felt my pain beyond me and never-ending prayers and support. I consider them as a divine of encouragement.

ABSTRACT

Nowadays, as global warming is becoming one of the world's most urgent problems, we need to find a better way to use energy, particularly in the energy storage are. Thermal energy storage is one of the recommended ways to improve energy recovery from solar energy, off-peak electricity and industrial waste heat recovery. In this paper, an overview of the Phase Change Material (PCM) experimental procedure is explored to improve its thermal conductivity. Enhancing PCM involves the use of nanoparticles that would influence the thermo-physical properties. Hence, the best candidate material as Nano fluids is preferred in order to maximize the thermal conductivity of the PCMs properties. The degree of super cooling of PCM affected by nanoparticle dispersion that can be regulated by the nanoparticle nucleation agent. In addition, the tiny structure can cause a large surface area of nanoparticles to correlate with their physical and chemical properties which lead with PCM's thermal-physical properties. Nanoparticles based on graphene are discussed in this study. The graphene surface area is the main characteristics used to determine the best thermal physical properties of material for Nano-enhanced phase change (NEPCM). Due to the best characteristics as base phase change material, inorganic salt hydrates material is reviewed in this paper. However, the use of graphene nanoparticles synthesis, characterization and modification process of nanoparticle itself to improve the thermal physical properties of inorganic PCM has been performed with limited research. The experiments in this paper are based on previous researchers by using different material of Nano fluids. The expected result of the study might be that the increasing percentage of thermal conductivity of the PCMs associated with its properties using systematic and numerical methods.

ABSTRAK

Pada masa kini, kerana pemanasan global menjadi salah satu masalah dunia yang paling mendesak, kita perlu mencari cara yang lebih baik untuk menggunakan tenaga, terutamanya dalam simpanan tenaga. Penyimpanan tenaga haba adalah salah satu cara yang disyorkan untuk meningkatkan pemulihan tenaga daripada tenaga suria, elektrik luar dan pemulihan haba sisa industri. Dalam makalah ini, gambaran keseluruhan proses eksperimen Bahan Perubahan Tahap (PCM) diuji untuk meningkatkan kekonduksian terma. Meningkatkan PCM melibatkan penggunaan nanopartikel yang akan mempengaruhi sifat fizikal terma. Oleh itu, bahan kandidat yang terbaik sebagai nanofluid adalah pilihan untuk memaksimumkan kekonduksian terma sifat-sifat PCM. Tahap Super cooling PCM dipengaruhi oleh penyebaran nanopartikel yang boleh dikawal oleh ejen nukleasi nanopartikel. Di samping itu, struktur kecil boleh menyebabkan luas permukaan nanopartikel yang besar untuk mengaitkan sifat-sifat fizikal dan kimia mereka yang membawa sifat-sifat fizikal haba PCM. Nanopartikel berdasarkan graphene dibincangkan dalam kajian ini. Kawasan permukaan graphene adalah ciri-ciri utama yang digunakan untuk menentukan sifat fizikal terma bahan terbaik untuk perubahan fasa nano yang dipertingkatkan (NEPCM). Oleh kerana ciri-ciri terbaik sebagai bahan perubahan fasa asas, bahan hidrat organik hidrat dikaji semula dalam kertas ini. Walau bagaimanapun, penggunaan sintesis nanopartikel graphene, pencirian dan pengubahsuaian nanopartikel itu sendiri untuk meningkatkan sifat fizikal terma PCM bukan organik telah dilakukan dengan penyelidikan yang terhad. Eksperimen-eksperimen dalam karya ini adalah berdasarkan penyelidik terdahulu dengan menggunakan bahan nanofluid yang berlainan. Hasil kajian yang diharapkan ialah peningkatan peratusan termal PCM yang dikaitkan dengan sifatnya menggunakan kaedah sistematik dan berangka.

ACKNOWLEDGEMENT

I should first like to take this opportunity to give my heartfelt thanks to Sir Mohd Noor Asril bin Saadun, my supervisor from the Faculty for Mechanical Engineering of Universití Teknikal Malaysia Melaka (UTeM) for his useful energy and time, and for his guidance, support and encouragement in the completion of this task.

I would also like to express great thanks for the advice, consultation and suggestions offered by my beloved friends at the Faculty of Mechanical Engineering, who has given me a clear idea of how the research project should take place.

Special thanks to Faculty of Mechanical Engineering, Universiti Teknikal Malaysia Melaka (UTeM) for the financial support throughout this project. Lastly, thank you to everyone who had been to the crucial parts of realization of this project.

TABLE OF CONTENTS

LIST OF TABLES

LIST OF TABLES

LIST OF TABLES

LIST OF FIGURES

LIST OF FIGURES

LIST OF FIGURES

LIST OF FIGURES

LIST OF ABBREVIATION

TES	Thermal Energy Storage
PCM	Phase Change Material
NPCM	Nano fluid Phase Change Material.
SSPCM	Shape Stabilized Phase Change Material
LHS	Latent Heat Storage
EG	Expanded Graphite
CN	Carbon Nano-additive
MWCNT	Multi-Walled Carbon Nanotubes
XGnP	Exfoliated Graphite Nano Platelets
R-GN	Random Graphite Nano sheets
0-GN	Oriented Distribution Graphite Nano sheets
T_m	Temperature Material
T_{mp}	Temperature Melting Point
T_{fp}	Temperature Freezing Point
DT	Temperature Difference
TEM	Transmission Electron Microscopy
SEM	Scanning Electron Microscopy

LIST OF ABBREVIATION

DSC	Differential Scanning Calorimetry
FT-IR	Fourier-Transform Infrared Spectroscopy
XRD	X-ray Powder Diffraction
PT100	Platinum Resistance Thermometers
$CaCl_2$	Anhydrous Calcium Chloride
γ-Al_2O_3	Gamma Aluminum Oxide
SiO_2	Silicon Dioxide
TiO_2	Titanium Dioxide
Cu	Copper
$CaCl_2H_2O$	Calcium Chloride Hexahydrate

CHAPTER 1

INTRODUCTION

1.1 Background of Study

The energy crisis is the concern that as demand rises, the demands of the world on the limited natural resources used to power industrial society are declining. The availability of these natural resources is minimal. While they do occur naturally, replenishing the stores will take hundreds of thousands of years. Governments and individuals concerned are seeking to promote the use of renewable resources and to reduce the unsustainable use of natural assets through growing conservation. There are many international efforts working to resolve the energy crisis. One of the ways and solutions to reduce the energy crisis is by thermal energy storage (TES) in the daily life application.

Thermal energy is an ancient resource that is commonly used energy in the world. Thermal energy storage is one of the recommended ways to improve energy recovery from the solar energy, off-peak electricity and industrial waste heat recovery. This system has a variety of uses such as for renewable energy source and as sensible latent heat source. Thermal energy storage system is greatly dependent in the requirement for its storage time which is divided as long term storage and short term storage. In another way, it is divided as sensible heat storage and latent heat storage. Normally, water is used as a storage medium for their sensible heat storage system.

The conservation of thermal energy using phase-change materials (PCMs) is of great interest in many fields such as solar energy systems, floor heating and energy-efficient houses. (Cheng et al, 2010). Thanks to their desirable properties such as high latent fusion energy and low vapor pressure during melting, the fatty acids and paraffin wax can be described as the organic PCMs that can be used. However, the difficulty of this organic PCMs which is paraffin is due to its low thermal conductivity (with an average of 0.2W/(m·K). Low thermal conductivity will reduce the rate of heat transfer during melting and solidification cycles. In addition, during the solid-liquid transition, paraffin is suffering from leakage. Studies of paraffin's effective encapsulation and enhancement of thermal conductivity are therefore of great importance. In this study, significant efforts have been made to boost the thermal conductivity of PCM with the approaches, including the introduction of various high thermal conductive additives to PCM, such as carbon nano-additives (CNs) and graphene nano-additives, where CNs are considered to be the most promising additives. Until now, most previous studies have focused on the enhancement of PCM thermal conductivity by single CN, summarized and compared in our previous study by (Qu et al, 2020).

A new concept of the use of nano-sized particles called nanofluids in various metals and metal oxides such as carbon nano-additives, copper nano-additives and graphene nano-additives has become commercially available. Nanoparticles ' heat transfer is boosted as size decreases as the surface-to-volume ratio boosts. The rising prevalence of thermal conductivity of paraffin has been followed by an increase in the heat transfer rate which also increases the loading and unloading time for paraffin. Addition of PCMs nanoparticles will enhanced their thermal conductivity.

This project is focusing on the rising of thermal conductivity with and without using nanoparticles. The effects of nanofluids on the performance of a phase change material (PCM) for thermal energy storage system will be determine by comparing the data from previous literature.

1.2 Problem Statement

Phase change materials (PCM) has gain attention for years as a suitable medium in the thermal energy storage system. One of the most common approach to increase the thermal conductivity and improving the thermos physical properties of PCM is by adding nanoparticles making it as nano-enhanced PCM. On the other hand, some PCM has disadvantages such as Super cooling and combustible that needs to be considered for further improvement is determined. The effect of nanofluids on the performances of phase change material (PCM) for the thermal energy storage will be determine in this project. Thermal analysis method among the way of how to determine the thermal conductivity of the phase change material (PCM). This project will be engaging in term of comparison data and experimental from the previous researchers.

1.3 Objective

The objectives of the project are as follows:

1. To determine the suitable material of nanoparticles in enhancing the phase change material thermo-physical properties.
2. To investigate the effect of latent heat of PCM by using different nanoparticle.

1.4 Scope

The addition of nano-additives on the PCMs will influence the thermal conductivity of the thermal energy storage system. The aim of this project is to discover the effect of nanofluids on the performance of PCMs of the thermal energy storage. The data are then will be used to calculate the efficiency of the thermal conductivity and latent heat value significantly. This research is initially with design process and demonstrate by experimentally. Only comparison data and experimentation from previous literature are involve in this project.

1.5 Hypothesis

This experiment aimed to investigate the thermal performance of nanofluid PCMs for TES system. The concern of this project is to improve and increase the efficiency of the thermal conductivity and the effect of latent heat for the energy storage system. In order to achieve the higher thermal conductivity, by introducing nano-additives such as carbon and graphene with the paraffin wax will be conducted. The data will be used to calculate the efficiency of the thermal conductivity of the phase change material (PCM) by using thermal analysis method.

CHAPTER 2

LITERATURE REVIEW

2.1 Thermal Energy Storage (TES)

In general, thermal energy storage (TES) and phase-changing materials in particular, has been a major research subject for the past 20 years. TES provides solutions in very specific areas (Zalba et al, 2003) such as the time delays and power availability between energy generation (solar energy, cogeneration, etc.), energy security (hospitals, data centres, etc.) and thermal inertia and thermal protection.. In 2003, Zalba gave a useful classification of the substances used for TES, shown in Figure 21..

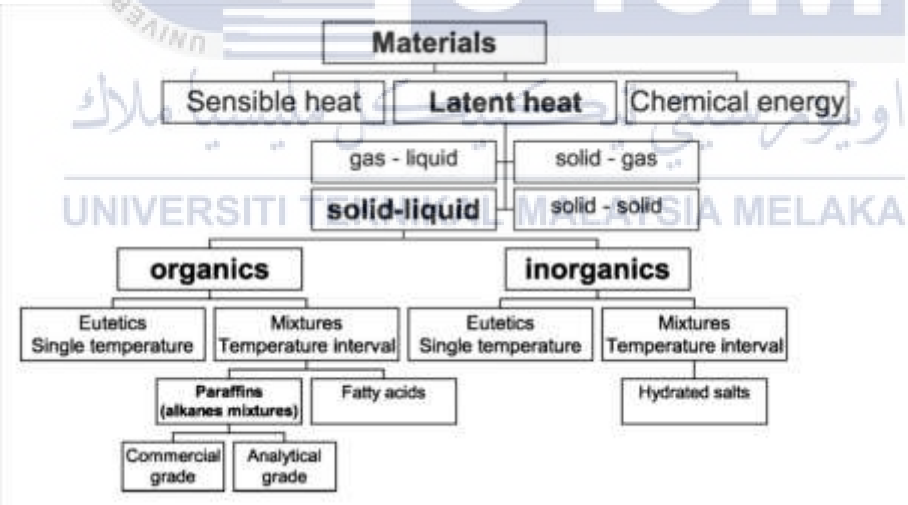

Figure 2.1 Classification of energy storage materials (Zalba et al., 2003).

These include a complete review of the types of materials used, their identification, properties, benefits and drawbacks, and the various testing methods used to assess the behavior of these materials in melting and solidification.

Energy demands in the commercial, manufacturing, service, and residential sectors vary every day, every week, and every season. The use of TES in such diverse sectors demands that the different TES systems operate synergistically and that they suit each particular application carefully. Much attention has recently been paid to the use of TES for thermal applications such as space heating, hot water heating, cooling, air conditioning, and so on. In industrial countries, a number of modern TES techniques have been developed over the past four or five decades (Dincer, 2002).

In all TES implementations, the principle is the same. The basic principle of TES system is to store energy through the process of absorption and release it for later use. At least three phases are involved in a complete storage process: charging processing and discharging as shown in Figure 2.2. The thermal energy storage mechanism is either by raising the temperature of a substance known as sensitive heat storage (SHS) or by adjusting the phase of a substance known as latent heat storage (LHS) or by combining these two types of heat storage methods (De Gracia & Cabeza, 2015).

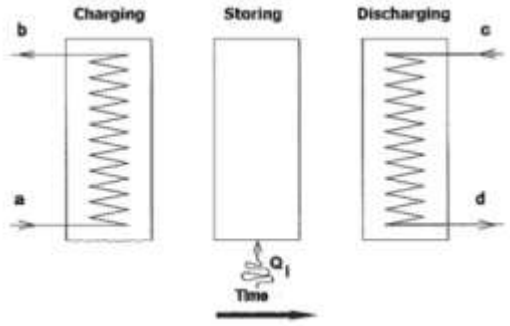

Figure 2.2 Basic principle of TES (De Gracia & Cabeza, 2015).

The three common heat storage materials used today are sensible heat storage, latent heat storage and chemical heat storage. However, because SHS has variable discharge temperatures and low energy density, compared to latent or thermo-chemical thermal energy storage, this method is not efficient. Therefore, LHS is the preferred method for storing thermal energy.

Although TES is used in a wide range of applications, all are designed to operate on a cyclical location (usually weekly, occasionally and seasonally). The devices achieve upper-range advantages that satisfy one or more of the following objectives. The first objective is to increase the capacity of generation. The second purpose is to allow cogeneration plants to operate in a variety of ways. Lastly, the purpose that need to be follow by the TES system to achieve benefits is by moving or shifting energy purchases to low-cost periods (Dincer, 2002).

Most practical TES systems using phase-change energy storage involve solutions of salts in water. Such systems are affiliated with several problems, including the following (Dincer, 2002). The first problem is that super-cooling of the PCM may take place, rather than crystallization with heat release. This problem can omit partly the addition of small crystals as nucleating agents. The second problem is that building a heat exchanger cap is difficult to deal with the agglomeration of varying sizes of crystals floating in the liquid.

2.2 Phase Change Material (PCM)

Phase Change Materials (PCMs) are materials that absorb or release large amounts of so-called ' latent ' heat while experiencing a change in their physical condition, i.e. from solid to liquid and vice versa In the fields of thermal energy storage and digital thermal management, phase change materials (PCMs) were used extensively due to their high phase change enthalpy,

stable chemical property, suitable and constant phase change temperature and low cost (Zheng et al, 2018). Table 2.1 shows the properties of PCM (Ali et al., 2019).

Table 2. 1 The properties of PCM (Ali et al., 2019).

Property	Value
Melting temperature (°C)	32
Freezing temperature (°C)	30
Latent heat (kJ/kg)	230
Liquid density (kg/m^3)	878
Solid density (kg/m^3)	906

(Mohamad & Che Sidik, 2019) notes that melting temperature and latent fusion heat are two components in the identification of the necessary phase change material (PCM) for latent heat storage Table 2.2 shown the classification of PCMs. Inorganic PCMs have greater enthalpy for phase changes, resulting in high thermal properties as shown in Table 2.3. Organics phase change materials such as paraffin's are widely used for thermal energy storage systems. In addition, inorganic PCMs vary in a number of important ways from organic PCMs.

Table 2. 2 Classification of PCMs (Mohamad & Che Sidik, 2019).

Phase Change Materials	Organic	Paraffin Compounds
		Non-Paraffin Compounds
	Inorganic	Salt Hydrate
		Metallics
	Eutectic	Organic-Organics
		Inorganic-Inorganic
		Inorganic-Organic

Table 2. 3 Comparison of organic and inorganic phase change materials (Mohamad & Che Sidik, 2019).

	Advantages	Disadvantages
Inorganic	Greater phase change enthalpy	Super cooling
	Higher energy storage density Higher thermal conductivity	Phase segregation
		Corrosive
	Non-flammable	Lack of thermal stability
	Inexpensive	
Organic	No corrosives	Lower phase change enthalpy
	Low or none Super cooling	Low thermal conductivity
	Chemical and thermal stability	Flammability

2.2.1 Classification of PCM

Based on their composition, PCM can be graded into organic, inorganic and eutectic as shown in Table 2.4. Zalba et al, (2003) defined and reported that the appropriate PCM is necessary to meet the system requirements.

Table 2. 4 Classification of PCM (Zalba et al., 2003).

Phase Change Material		
Organic	**Inorganic**	**Eutectic**
1. Paraffin	1. Salt Hydrate	1. Organic
2. Non-paraffin	2. Metallic	2. Inorganic-Inorganic
		3. Inorganic-Organic

Organic materials such as glycerine and vinyl stearate are divided into paraffins and non-paraffins. Because of the existence of the long carbon chain, it can absorb or release large amounts of latent heat. The paraffin PCM can be used regularly and is non-corrosive and non-sub-cooling due to its high chemical stability. However, the major disadvantage of organic PCMs is its low thermal conductivity. Organic non-paraffin PCM is similar to paraffin PCM but is relatively corrosive, costlier and highly inflammable (Wu et al, 2009).

Due to its higher density, inorganic PCM has higher latent heat per unit mass. It has higher heat conductivity (about 0.5W / m ° C), less flammable, lower toxicity, more corrosive and cheaper than natural PCM. Based on inorganic salts such as calcium chloride hexahydrate ($CaCl_2H_2O$), salt hydrate is formed by mixing the water. The salt hydrate PCM, however, is

vulnerable to subcooling and separation of the process. The metallic inorganic PCM contains the component of metal alloy, exhibits higher heat fusion per unit volume and thermal conductivity. On the other hand, it shows low fusion of heat by weight, low specific heat efficiency and vapor pressure (Khanafer, Vafai, & Lightstone, 2003).

2.2.2 Latent heat

Latent heat is the energy that a material absorbs or releases during a change in temperature. The process is either a transition from a solid to a liquid or a gas or the other way around. As shown in Figure 2.3, absorbing or charging energy from the surrounding environment or warmer material to the substance can cause the molecules to disperse into a greater phase size, i.e. solid into liquid phase change. In other words, a lower-density material gives off energy or discharge to change a phase of higher density, as the molecules come closer together and lose energy from motion and vibration (Sidik et al., 2018).

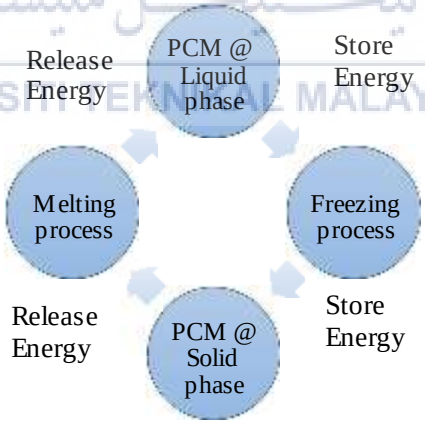

Figure 2. 3 Solid-liquid-solid phase change cycle (Sidik et al., 2018).

Phase change content is widely used in the latent heat storage (LHS) process as a heat storage medium consisting of storage capacity as below formula.

$$Q = m\left[C_{sp}(T_m - T_i) + a_m \Delta h_m + C_{lp}(T_f - T_m)\right] \quad (1)$$

The benefit of PCM in the latent heat storage system as shown in Figure 2.4 is a constant temperature between absorption and release of energy. Furthermore, it is possible to store energy per unit per volume 5-14 times more than responsive storage materials. Generally speaking, LHS has low cost of capital, higher density of storage and low loss of energy to the environment. The main disadvantages of LHS materials, however, are corrosive to metallic walls and their phase segregation could lead to super cooling. The three key basic criteria for the LHS system are appropriate temperature range of phase change materials (PCM) , storage containment system and heat exchange mechanism (Kibria et al, 2015).

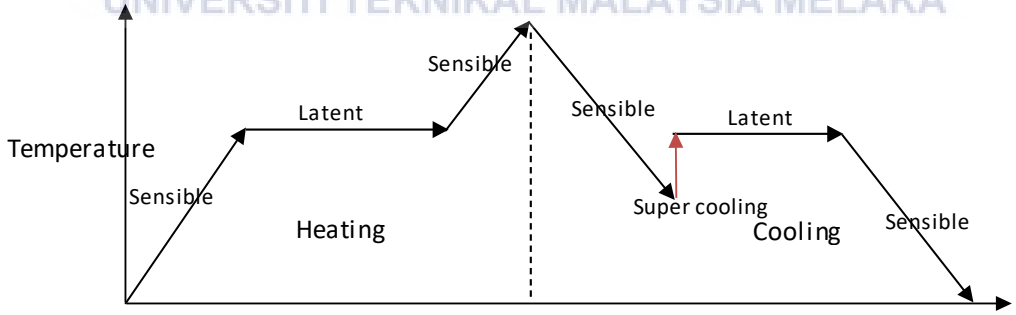

Figure 2. 4 Sensible and latent heat phase change for solid-liquid-gas (Kibria et al., 2015).

2.2.3 Melting

Heat is added to the PCM during the melting cycle for the first time and later for the natural convection. This is because the solid area shifts away from the surface of heat transfer and the thickness of the region of liquid rises close to the surface of heat transfer. Since the thermal conductivity of liquid PCM is less than the thermal conductivity of solid PCM, as the melting process continues, the heat transfer is almost negligible. The further fusion is mostly due to the gradient of density within the liquid PCM (Jegadheeswaran & Pohekar, 2009).

2.2.4 Solidification

Contrary to the phase of melting, solidification is regulated by conduction. Natural convection only occurs in the case of solidification and, as time goes on, the effect of natural convection is almost negligible relative to the effect of convectionSeveral researchers have clarified the heat transfer characteristics of PCM during solidification (Jegadheeswaran & Pohekar, 2009).

2.2.5 Super cooling

As described in the previous chapter, salt hydrate as inorganic PCM has superior properties such as better thermal conductivity, higher latent fusion energy, and lower prices for their organic counterparts. Nevertheless, in their applications for thermal energy storage, their intense Super cooling during freezing and phase isolation during melting led to challenges. Therefore, adding any chemistry nucleating agent is the most frequently used way to render the Super cooling change. In theory, the optimal nucleating agents should be identical to the base materials lattice parameter. For example, Borax is always notable as the most acceptable nucleating agents for inorganic salt hydrated $Na_2SO_4.10H_2O$, which can decrease the degree of Super cooling about 12°C ~13°C (Mohamad & Che Sidik, 2019).

The Super cooling problem can be solved successfully by the addition of borax (Na2B40r.lOHrO) as a nucleating agent. Several different thickening agents have been studied, including organic such as starch, alginates, and various types of cellulosic mixtures, as well as inorganic substances such as silica gel and diatomaceous earth. Many organic substances are gradually hydrolyzed or decomposed by bacterial or enzyme activity, and some of the silica materials resist borax nucleation. Glauber's salt mixture with attapulgite clay and borax significantly improves the prevention of phase separation (Shin et al, 1989) .

2.2.6 Materials

Paraffins are generally the most commonly used organic PCMs. Paraffin, a traditional organic material for phase change, has been widely used due to its many advantages including non-toxicity, stable chemical properties, no phase separation, low volume changes during the phase change cycle, high enthalpy and low cost (Zheng et al., 2018). Although, paraffin's poor

thermal conductivity (approximately 0.24 W / m·K) limits its widespread use due to inefficient heat transfer when thermal energy is consumed or released. To improve the thermal performance of paraffin as a PCM, its low conductivity should be improved by impregnating with expanded graphite(EG) or aluminum and nickel foams, or mixed with these metals ' fibers and fillers are typical examples of such composites and are promising to increase heat transfer. (Kahwaji et al, 2018). Table 2.5 contains the physical properties of paraffin wax.

Table 2. 5 shows the properties of paraffin wax (Kahwaji et al., 2018).

Melting point	56.06 °C
Density of the PCM (liquid Phase)	775 kg/m^3
Density of the PCM (solid phase)	833.60kg/m^3
Specific heat of solid (< 30 °C)	2.565 J/g °C
Specific heat of liquid (> 65 °C)	2.439 J/g °C
Flash Point	199 °C

Graphite is a crystalline form of the carbon element with its hexagonally arranged atoms. This occurs naturally in this form and under standard conditions it is the most stable form of carbon. For their high thermal conductivity or excellent mechanical properties, carbon-based materials are commonly used. In order to improve the thermal management of thermal energy storage (TES), the effects on thermal conductivity and shape stability of nano-graphite sheet charging on paraffin are investigated (Chang et al, 2017). Researchers reported that paraffin thermal conductivity mixed with nano-graphite sheets of 15 wt percent was improved by five times compared to pure paraffin sheets, and paraffin / nano-graphite sheets showed higher shape-stabilized properties. Furthermore, expanded graphite (EG) was recognized for its low

density, high porosity, high thermal conductivity, low price and compatibility with organic phase-change materials (Zhang & Fang, 2006). The incorporation of EG into paraffin could increase its thermal conductivity significantly and improve the efficiency of thermal transfer. Porous EG could also be used as a carrier to absorb PCM into a stabilized phase change material (SSPCM), which could then prevent paraffin leakage during the melting process.

2.3 Composite's Material

A composite material made of a carbon-based matrix (high thermal conductivity) and PCM (high energy storage) were formed to overcome the low thermal conductivity. Certain types of techniques to boost thermal conductivity of PCMs are shown in existing literature, where paraffin is used as PCM. These include the encapsulation of paraffin and the blending into the liquid paraffin of extended graphite. Paraffin was selected among all PCMs because of its high latent heat, good thermal and chemical stability and low cost (Gilart et al, 2012).

2.4 Nanofluids

In many industrial sectors, heat transfer fluids such as water, minerals oil and ethylene glycol play an important role, including power generation, chemical processing, air conditioning, transport and microelectronics. Also, their low thermal conductivities limit the efficiency of these traditional heat transfer fluids. Growth of high-performance heat transfer fluids has been the subject of numerous investigations in recent decades, depending on the industrial needs of system intensification and device miniaturization (Wong & De Leon, 2010). It is well known that metallic solids have a higher thermal conductivity at room temperature than liquids in order of magnitude. Copper's thermal conductivity at room temperature, for example, is about 700 times that of water and about 3000 times that of engine oil. The thermal

conductivity of fluids containing suspended metallic or non-metallic (metallic oxide) particles would therefore be required to be substantially higher than that of standard heat transfer fluids. (Wu et al., 2009).

Suspending various types of small solid particles such as metallic, non-metallic and polymeric particles in traditional fluids to form colloidal is an innovative way to improve the heat transfer efficiency of specific fluids. Nevertheless, suspended particles of the order of μm (micrometer) or even mm (millimeter) that cause some pro-related elements in the flow channels, causing the particles to settle out of suspension quickly. Modern nanotechnology has been discovered in recent years. Particles of the dimensions of nanometers dispersed in any liquid are called nanofluids. Compared to particle suspensions of a millimeter or micrometer scale, nanofluids have demonstrated a number of potential advantages such as long-term staffing and rheological properties and can have significantly higher thermal conductivity.

2.4.1 Type and Application of Nanofluids

Some of the nanoparticles used in nanofluids include oxide ceramics (Al_2O_3, CuO, Cu_2O), nitride ceramics (AIN, SiN), single, double or multi-walled car composite materials (SWCNT, DWCNT, MWCNT), and composite materials such as core polymer shell composites. Furthermore, the use of new materials and structures in nanofluids where the particle-liquid interface is doped with different molecules is attractive. Liquids used in nanofluids such as water, engine oil, ethylene glycol and ethanol are typical heat transfer fluids (Shanthi et al, 2012).

Nanofluids can give numerous benefits when the nanoparticles are adequately distributed, apart from the anomalously high active thermal conductivity. These properties

provide improved heat transfer and stationary efficiency. Since heat transfer takes place on the particle surface, the use of particles with a larger surface area is preferable (Manca, Jaluria, & Poulikakos, 2010). Compared to microparticles, the relatively larger surface area of nanoparticles provides significant increases in the capacities for heat transfer. Furthermore, particles below 20 nm bear 20% of their atoms on their surface, making them available for thermal interaction immediately. Nanofluids can flow smoothly in the tiniest of channels like mini- or microchannels with such ultra-fine particles. Since the nanoparticles are small, gravity is less important and therefore the chances of sedimentation are also lower, making nanofluids more stable.

Microchannel cooling without clogging: Nanofluids will not only be a heat transfer medium in general, but they will also be suitable for microchannel applications where high heat loads are identified. The combination of microchannels and nanofluids will provide a large area of heat transfer and highly conductive liquids. This cannot be done with macro- or micro-particles because micro-channels are clogged.

Miniaturized systems: Nanofluid technology will support the current industrial trend towards miniaturization of components and systems, including the development of smaller and lighter heat exchanger systems. Miniaturized devices can reduce the heat transfer fluid stock and contribute to cost savings.

Reduction in pumping power: In order to increase traditional fluid heat, transfer by a factor of two, the pumping power usually has to be increased by a factor of ten. Without a sharp increase in fluid viscosity, the required increase in pumping power will be very mild. Using a small volume fraction of nanoparticles, very large savings in pumping energy can be achieved if a large increase in thermal conductivity can be achieved. Nanofluid stability will prevent rapid

settlement and decrease clogging in the heat transfer device walls. Nanofluid's high thermal conductivity translates into increased energy efficiency, upper performance, and lower operating costs. In order to pump heat transfer fluids, they can reduce energy consumption. Miniaturized systems require smaller inventories of fluids where it is possible to use nanofluids. Thermal systems are likely to be smaller and lighter. Smaller components result in fuel savings, reduced emissions and a cleaner environment in vehicles. (Manca et al., 2010).

2.4.2 Natural Convection of Nanofluids and Heat Transfer Solution Approaches

In many applications in the chemical industry, food industry and also in solar collectors, the natural convection of liquid small-particles suspensions has been used. Similar to that of pure liquids, the normal convection of suspensions is special. The natural convection of a suspension is driven by the unpredictable distribution of fluid density due to differences in temperature and the distribution of particle size due to sedimentation (Kang et al, 2001).

Because of the lack of experimental data on natural nanofluid convection, an analytical model was developed by (Khanafer et al., 2003) to determine the natural convective heat transfer of nanofluids. In a single phase, the nanofluid in the enclosure was believed to be equal, i.e. the fluid and particles are at the same velocity in thermal equilirium and flow. The effect of suspended nanoparticles on the heat transfer process driven by some buoyancy has been analyzed. It was shown that the heat transfer rate increased as the fraction of the particle volume increased at any given Grashof number (Gr).

Xuan and Roetzel, (2000) used two approaches to derive some correlations to predict convective heat transfer of nanofluids. Nanofluids were treated as a single phase fluid by the first approach and the other as a solid-liquid mix. The derived correlations demonstrated that

the nanofluid heat transfer enhancement mechanism depended on the increasing thermal conductivity of the suspension and the chaotic particle motion that accelerates the fluid energy exchange cycle. Furthermore, to test this model, there is still a lack of experimental research.

Afterwards, Xuan & Li, (2000) proposed a nanofluid convective heat transfer and flow characteristic experimental investigation. A Cu-water nanofluid was used in their experiments with particle concentrations ranging between 0.3 and 2 percent volume fraction and flows occurring in a straight tube The results showed that the suspended nanoparticles increased the heat transfer of the ase liquid, and the nanofluid convective heat transfer coefficients increased with increased flow rate and concentration of particles. The greater increase in heat transfer was found to be more than 39 percent at a fraction of 2 percent particle density. In addition, nanofluids did not cause any major pressure drop change.

2.5 Type of Analysis

They are many type of analysis used for conducting experiment related to Nano-fluid PCMs such as TEM analysis (Kajita, S. et al,2012), DSC analysis (Drissi, S.et al, 2015), FT-IR analysis (Karaipekli, A. et al, 2009) and XRD analysis (Hassan Y. et al, 2015).

(Kajita, S. et al,2012) TEM analysis (or TEM testing) uses high-energy electrons (usually 100-300kV), which are transmitted by a transparent electron sample. A TEM makes use of these high-energy electrons to create an image instead of using visible light. To image a sample in the TEM, the sample must be thin enough to be transparent to the electron (approximately 80-100 nm thick). That is not a problem for samples of nanoparticles. That is because nanoparticles have relatively small (1 to 100 nm) diameters.

(Drissi, S.et al, 2015) The Differential Scanning Calorimeter (DSC) technique was used to characterize thermal character of both damaged and non-damaged PCMs. The DSC technique is useful in determining many of a material's thermodynamic properties, such as melting and freezing temperatures, unique heat, phase change enthalpies, etc. Consequently, several investigations were carried out using different dynamic levels and sample masses to optimize the experimental parameters which control the DSC test. (Sarı, A. et al, 2009) DSC is a technique that gives considerably precision to the accurate and reproducible tests.

FTIR analysis was also performed to determine the thermal and chemical stability of composite PCM after thermal cycling (Karaipekli, A. et al., 2009). Fourier Transform Infrared Spectroscopy, also referred to as FTIR Analysis, is an analytical technique used to identify organic, polymeric, and inorganic materials in some cases. The FTIR method of analysis uses infrared light to scan samples and to observe chemical properties.

X-Ray Diffraction, also abbreviated as XRD, is a non-destructive research tool used for the study of crystalline material structure (Hassan Y. et al, 2015). Through the study of the crystal structure, XRD analyzes are used to identify the crystalline phases present in a material and thus to reveal information on the chemical composition. X-ray diffraction (XRD) is an effective, non-destructive technique for crystalline material characterization. It provides information on structures, phases, desired crystal orientations (texture), and other structural parameters such as mean grain size, crystallinity, strain, and crystal defects.

2.6 Thermal Conductivity

Most paraffin has low thermal conductivity (with an average of 0.2W/(m·K)) which reduces the rate of heat transfer during the melting and solidification cycles. Furthermore, during the solid-liquid transition, paraffin suffers from leakage. Studies of paraffin's effective encapsulation and enhancement of thermal conductivity are therefore of great importance. Significant efforts have been made to improve the thermal conductivity of PCM with approaches including the addition of various high thermal conductive additives to PCM, such as carbon nano-additives (CNs), which are considered to be the most promising additives (Qu et al, 2020). Adding CNs can improve thermal conductivity and further enhance the stability of the Shape Stabilized Phase Change Material (SSPCM).

The most critical parameter for the PCM is thermal conductivity. As mentioned earlier, paraffin with low thermal conductivity can increase the response time of latent heat melting and freezing. Improving thermal conductivity is therefore an important parameter in product design processes. The thermal conductivity of the composites could be further improved by adding EG due to the high thermal conductivity of EG. The EG was therefore chosen to boost the conductivity of the PCM composites (Cheng et al., 2017).

The unique characteristics of nanofluids are a significant increase in liquid thermal conductivity, liquid viscosity, and heat transfer coefficient. It is well known that metals in solid phase at room temperature have higher thermal conductivity than fluids. (Kreith et al, 2010). Several methods have been tried to improve heat transfer in these PCMs in order to solve the low thermal conductivity issue of stabilized PCMs.

CHAPTER 3

METHODOLOGY

3.1 Overview of Research Methodology

This chapter describes the method involved in this project, which consists of the preparation and fabricate of phase change material (PCM) based on previous researchers. Below is a description of the research activities in this project as shown in Figure 3.1.

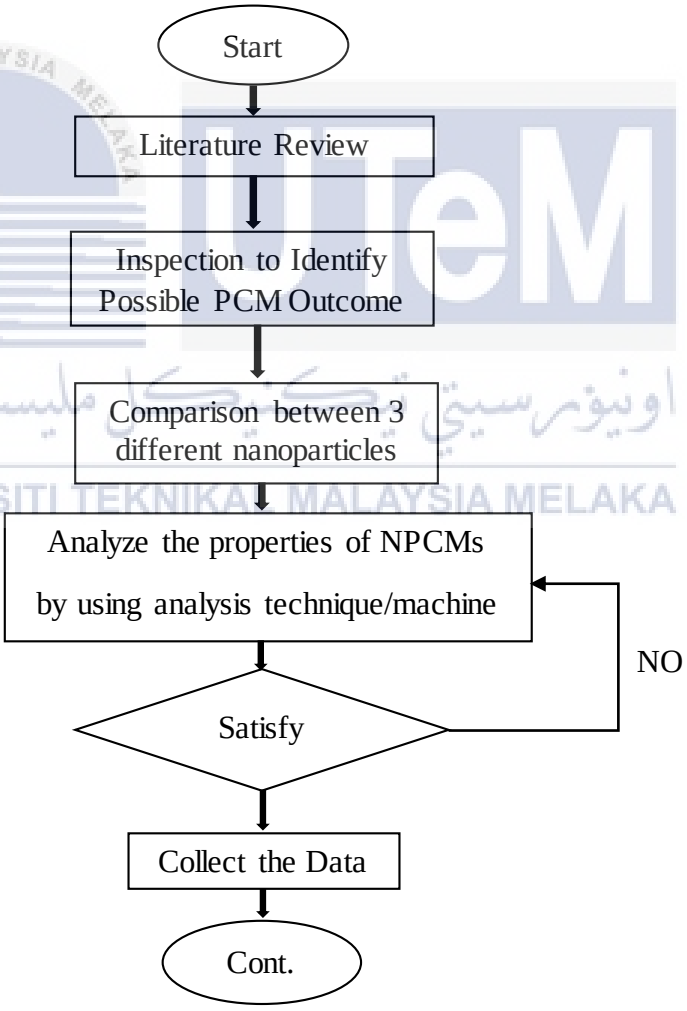

Figure 3.1: Flow chart of project research

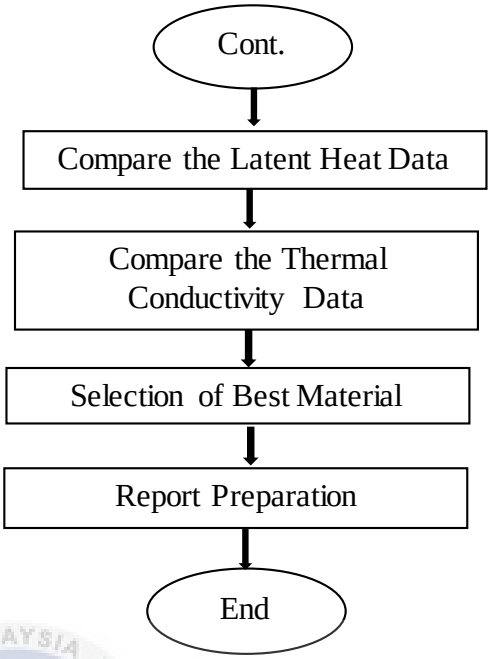

Figure 3.1: Flow chart of project research (Cont.).

3.2 Material

Material used in this experiment based on the previous researchers. The first experiment conducted by Murugan et al., (2018) use multi-walled carbon nanotubes (MWCNTs) as nano reinforcement in enhancing thermal conductivities of PCMs properties. The PCM and MWCNT requirements used in this investigation are outlined in this paragraph. (a) Paraffin with a melting temperature range of 18°C –23°C and a solidification range of 22°C –19°C is used as the base material in the preparation of the NPCM. The 53°C –59°C phase-changing paraffin is required for building heating applications and therefore the commercially available paraffin is selected as the base PCM. (b) Procurement of MWCNTs. MWCNT's average diameter, length and target area is 30–50 nm, 10–0 lm and 60 m2 g, respectively. MWCNT's thermo-physical properties are set out in Table 3.1. The Hitachi H-7500 transmission electron microscope as shown in Figure 3.2 is used in this experiment. It is suitable instrument for the investigation of high magnification of biological material. This particular TEM column design allows users to view

specimens at magnifications ranging from very low (700x) to very high (200,000x) while maintaining high resolution, wide field of view (160 mm) and high contrast.

Table 3. 1 MWCNT's thermos physical properties (Murugan et al., 2018).

Parameter	Value
Outer tube diameter	30–50 nm
Inner tube diameter	5–10 nm
Length	10–20 nm
Specific surface area	60 m2 g/1
True density	2.1 g/cm^3
Bulk density	0.28 g/cm^3
Electrical conductivity	>100 S cm
Purity	>95 wt. %

Figure 3.2: The Hitachi H-7500 transmission electron microscope.

For the second experiment which is conducted by Li et al., (2017) stated that the used of anhydrous calcium chloride ($CaCl_2$, purity>96%) as the main material. Gamma aluminum oxide (γ-Al_2O_3, 50nm, purity >99.9%), silicon dioxide (SiO_2, 50nm, purity >99.9%), titanium dioxide (TiO_2, 50nm, purity >99.9%), and copper (Cu, 50nm, purity >99.9%) nanoparticles were also used in his experiment.

Lastly, Cheng et al, (2017) conduct an experiment to fabricate the lightweight wall material with expanded graphite (EG)/paraffin composites. They stated that the raw materials used in the preparation of the wall material are based on fly ash, expanded graphite, paraffin, alkali and vesicant. Fly ash was the main raw material used. As supporting material, expanded graphite (EG) was used. Paraffin was used as fuel for thermal storage. Alkali activator (water glass, MS = 1.6, complex alkali activator) is prepared using certain proportions to mix water glass (MS = 2.4) with NaOH (1 mol / L).

3.3 Sample Preparation

Sample preparation is based on previous researchers which is involve different material of nanofluids. First and foremost, the preparation of PCMs used in the first experiment inspired the preparation process of nano-PCM. PCM's melting point is an important factor in determining the process for preparing the nano-PCM. Murugan et al., (2018) stated that nano-PCM with paraffin has a melting temperature range of 18°C–23°C and a solidification range of 22°C–19°C as the correct base material to be prepared as shown in the Figure 3.3 schematic diagram. Figure 3.4 displays the carbon nanotubes image of the transmission electron microscope (TEM), and some areas of the image note the existence of entanglements.

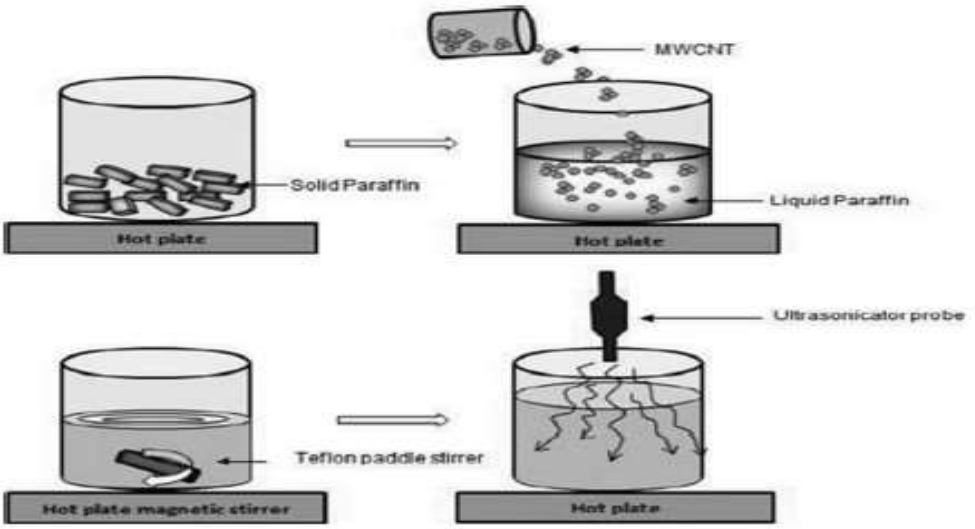

Figure 3.3: Schematic diagram of Nano-PCM preparation method (Murugan et al., 2018).

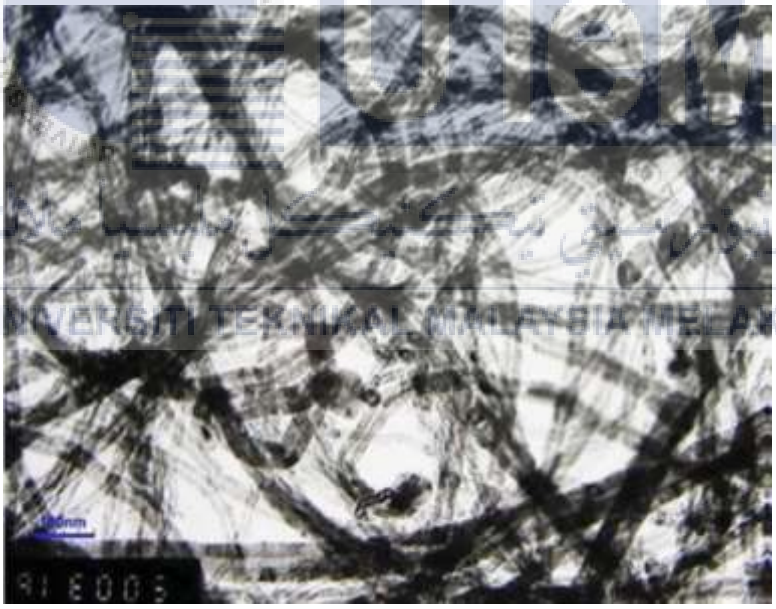

Figure 3.4: MWCNT TEM photo (source: Cheap Tubes, United States).

The nanotubes were ultra-sonicated under dry condition for 90 min to disentangle them. A novel two-step process for planning the NPCM is adopted. The MWCNT is homogeneously distributed in liquid paraffin using a 60-minute magnetic stirrer. Different specimens are prepared at concentrations of 0.3%, 0.6% and 0.9% of MWCNT, with the specificity that no dispersants of surfactants are used to achieve a stable suspension. The NPCM is continuously sonicated for 30 minutes in an ultrasonic bath, always maintained at a steady temperature of 30°C to ensure the samples are kept above the melting point of the paraffin. The NPCM scanning electron microscopy (SEM) image is collected at an accelerating voltage of 5 kV using a scanning electron microscope (H-7500). As shown in Figure 3.5, the average length of dispersed MWCNT varies from 32 to 46 nm in diameter.

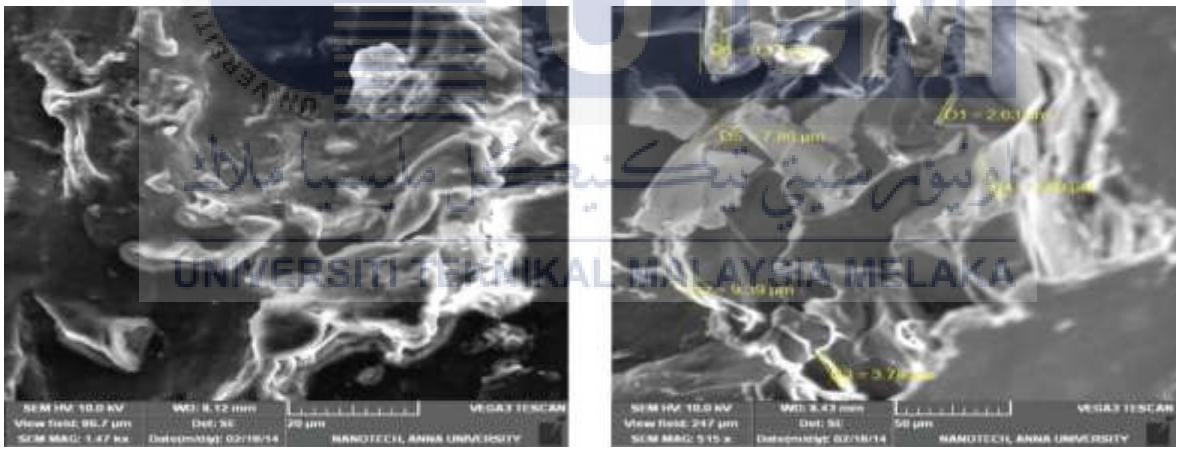

Figure 3.5: SEM image of the MWCNT dispersed.

Next, recent studies published by Li et al., (2017) also support this two-step nano-PCM preparation process with the application as the base material of inorganic salt hydrate. The product derived from $CaCl_2.6H_2O$ was dissolved and the commercial grade of $CaCl_2.6H_2O$ was crystallized. The research also used the two-step method of preparation for $CaCl_2.6H_2O$ nanocomposite PCMs. A magnetic stirrer with added surfactant and nucleating agent, $SrCl_2.6H_2O$ at 50°C for 20 min, was used to stir the solution homogenously. Stir the nanoparticles continuously for 10 min. Finally, ultrasonic vibration was applied to the preparation processes for another 30 min in order to ensure the dispersion stability of the mixture and minimize the separation and aggregation of nanoparticles. $CaCl_2.6H_2O$ nanocomposite PCM's schematic preparation is shown in Figure 3.6. This approach is the best and most popular form of preparation for PCM based on the analysis of the current study.

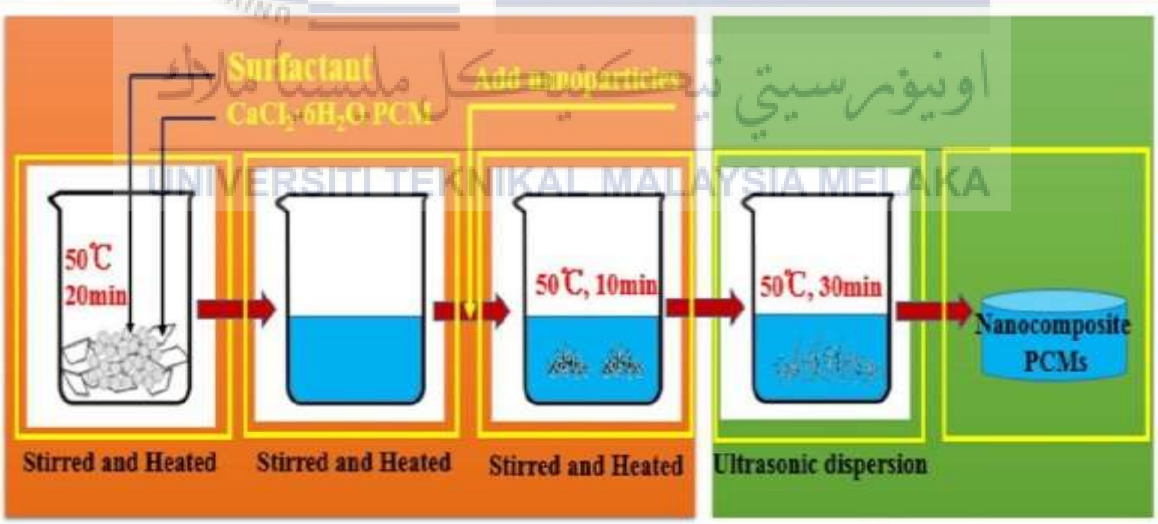

Figure 3.6: Schematic preparation of $CaCl_2.6H_2O$ nanocomposite PCMs (Li et al., 2017).

Table 3. 2 The compositions of the $CaCl_2.6H_2O$ nanocomposites *(Li et al., 2017).*

	Nanoparticle (wt.%)				Surfactant (wt.%)			
	Al_2O_3	TiO_2	Cu	SiO_2	SDBS	SDS	Span-80	CTAB
No.1	0.5	—	—	—	—	—	—	—
No.2	—	0.5	—	—	—	—	—	—
No.3	—	—	0.5	—	—	—	—	—
No.4	—	—	—	0.5	—	—	—	—
No.5	0.5	—	—	—	1	—	—	—
No.6	0.5	—	—	—	—	1	—	—
No.7	0.5	—	—	—	—	—	1	—
No.8	0.5	—	—	—	—	—	—	1
No.9	1.0	—	—	—	—	—	—	1
No.10	1.5	—	—	—	—	—	—	1
No.11	2.0	—	—	—	—	—	—	1
No.12	2.5	—	—	—	—	—	—	1

Lastly, Cheng et al., (2017) stated the preparation and analysis of lightweight wall material using expanded graphite (EG)/paraffin composites. The wall materials preparation process is split into two sections that are the preparation of EG / paraffin composites and foam concrete. The EG / paraffin composites were prepared using a mass ratio of 1:6, EG and previously melted paraffin were uniformly mixed and then moved for 90 min to an 80°C vacuum drying oven to allow paraffin to be absorbed into EG. The composites of EG / paraffin were then collected, placed on a double filter paper and dried on a constant 80°C oven. The specimen stayed in the oven until complete absorption of redundant paraffin.

Foam concrete was prepared as follows: suitable quantities of fly ash were milled by ball grinding equipment and processed into small particles, then divided into 5 classes of 120 g each graded from S1 to S5. The prepared EG / paraffin composites were subsequently applied to each class S1–S5 using ratios of 0%, 5%, 10%, 15% and 20%. Water was applied at a ratio of 0.67 (water / ash) and additional components were added to form a foam concrete: some water glass (MS = 1.6), ZC-41 vesicant foam (0.5 g) and liquid (19.5 g) combined with a foaming system. The resulting foam concrete was then poured into a 40 mm 40 mm 40 mm triple mold. The sample was taken out of the triple mold after 24 h and put in an air drying oven. The composites obtained are gradually stirred to create a uniform slurry by adding new material. Finally, they were put in a curing box under a steady 25 C temperature in order to obtain samples with stable properties. Table 3.3 shows the thermal conductivities of the groups S1–S5. The procedure is shown in Figure 3.7. Figure 3.8 shows the SEM images of the lightweight wall material with and without EG/paraffin composites.

Table 3. 3 Thermal conductivities of the groups S1–S5 (Cheng et al., 2017).

Experiment group	Content of EG/paraffin composites (%)	a 10^6 (m^2/s)	q 10^3 (kg/m^3)	Cp 10^3 [J/(kg K)]	k [W(m K)]
S1	0	0.288	0.401	3.31	0.39
S2	5	0.309	0.429	3.21	0.43
S3	10	0.362	0.438	3.09	0.49
S4	15	0.514	0.452	2.98	0.69
S5	20	0.573	0.471	2.82	0.76

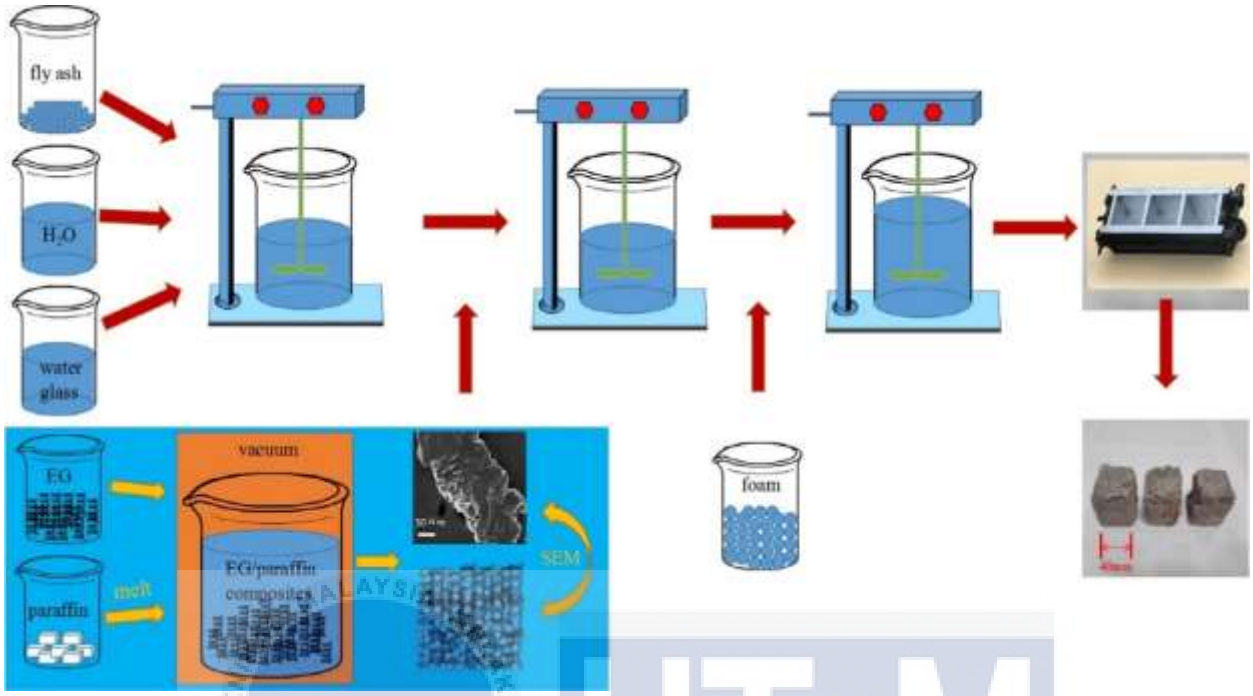

Figure 3.7: Preparation of EG/paraffin composites (Cheng et al., 2017).

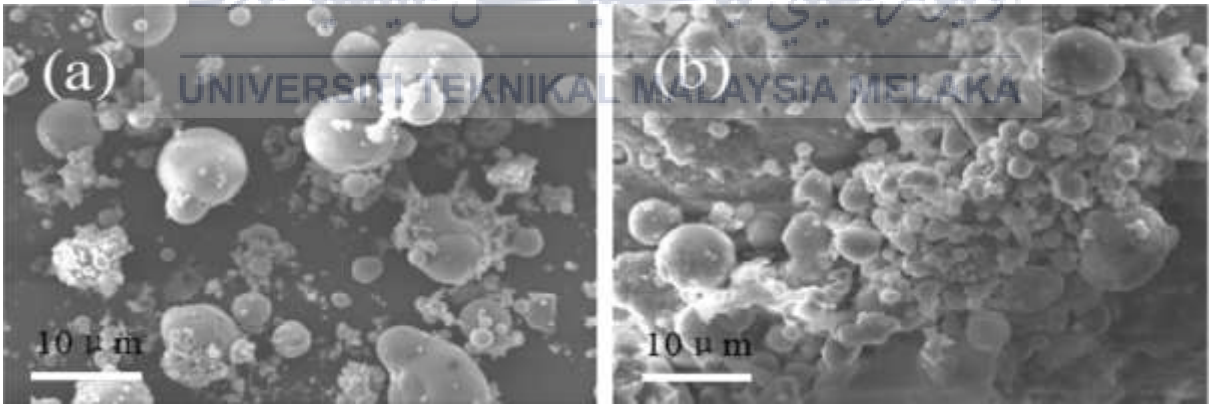

Figure 3.8 SEM images of the lightweight wall material. (a) Analysis without combination of EG / paraffin. (b) a sample of 15% EG / paraffin composite material (Cheng et al., 2017).

3.4 Experimental Energy Storage Test

(TingXian Li et al, 2014) Figure 3.9 shows the schematic diagram of working principle of the experimental system utilizing stearic acid with various carbon additives for phase shift nanocomposites. The experimental test system consists primarily of a thermostatic water bath at low temperatures, a thermostatic water bath at high temperatures, a heat storage tank, two flow meters, a data logger and several regulated valves. Latent heat storage nanocomposite is filled in the heat storage tank and its working temperature is controlled automatically by the two thermostatic water baths with a precision of 0.1°C using an electric heater and a compressor chiller. During the charging process, the heat absorbed by the phase change nanocomposite is supplied by the hot water from the high-temperature thermostatic water bath; while during the discharge cycle, the heat emitted by the phase change nanocomposite is collected by the cooling water from the thermostatic low-temperature water bath.

Two flow meters with an accuracy of 1.5% are used to calculate the mass flow of circulating water during the charging and discharge phases to define the thermal efficiency of these latent heat storage nanocomposites. To measure the temperature of phase change nanocomposite, three thermocouples are mounted in the heat storage tank and the installation location of the thermocouples is shown in Figure 3.10 (TingXian Li et al, 2014). The inlet and outlet water temperatures are measured using two thermocouples. The temperature measurement error is within ±0.5°C by using a PT100 platinum resistance sensor of four-wire type. The thermostatic water baths and the heat storage tank are insulated to reduce the ambient heat losses.

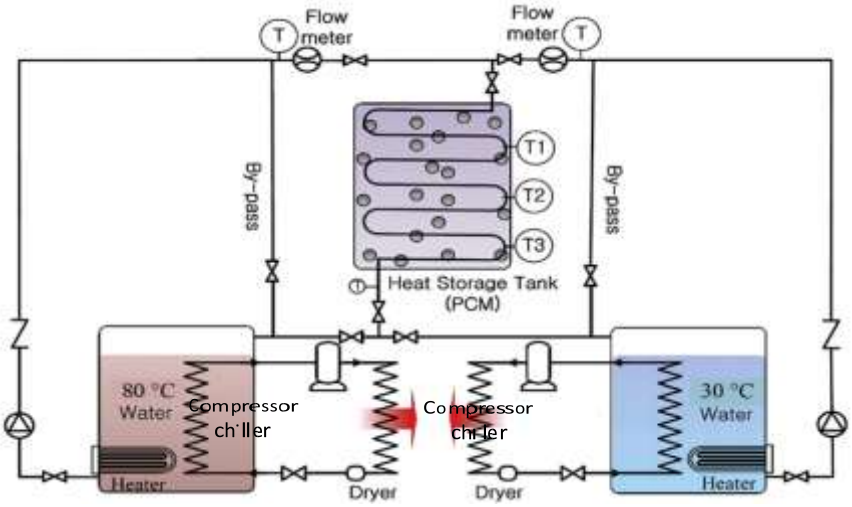

Figure 3.9: Schematic diagram of working principle of the experimental system (TingXian Li et al, 2014).

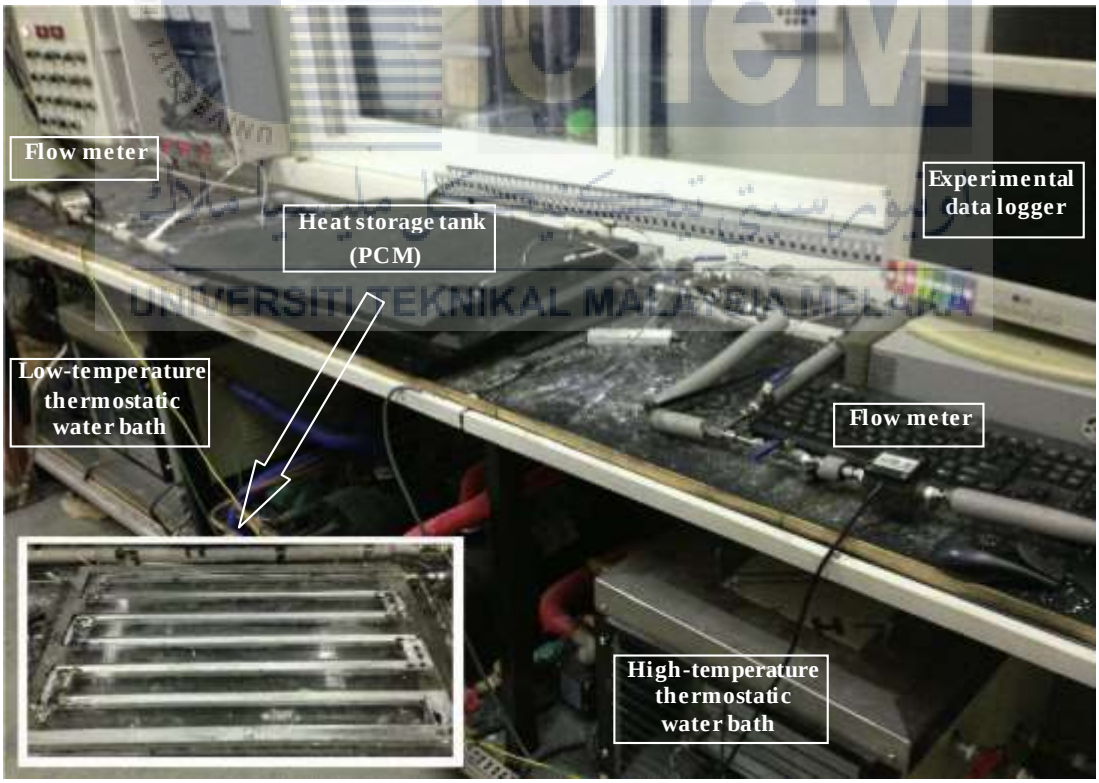

Figure 3.10: Photograph of the experimental system (TingXian Li et al, 2014).

CHAPTER 4

RESULT AND DISCUSSION

4.1 Introduction

Based in the literature review, it is crucial for an TES, as an interconnect material, to exhibit good thermal conductivity as well as high thermal efficiency of the material. Therefore, in this chapter, based on the previous experimental conduct by previous researchers in this study will be evaluate and be discuss in detail. The results are correlated with those attained PCM by using similar materials (with different combination of Nano fluids such as MWCNT, Cu, $CaCl_2.6H_2O$, γ-Al_2O_3, ,TiO_2, graphene particles) from previous research's.

4.2 First Experiment

For the first experiment conducted by (Murugan P et al, 2017), the pure PCM is used with MWCNT to increase the thermal conductivity of the PCM. Paraffin (Tm = 58°C – 60°C) was used as PCMs in the preparation of composite PCMs. Table 4.1 below shows the thermal conductivity and the similarities of the use of MWCNT particles by the previous researcher's.

(Li-Wu Fan et al, 2013) The melting temperature of the pure paraffin wax is 58.8°C, and is marginally lowered due to the presence of all the four types of carbon Nano fillers. There is, however, a lack of a clear relationship between the variation of the melting temperature and the loading of the carbon Nano fillers. The maximum change on the melting temperature is 0.75°C. Since the carbon Nano fillers do not melt/solidify in the temperature range of interest, the phase change enthalpies of the nanocomposite PCMs are expected to be somewhat lowered from those

of pure paraffin wax. At the highest loading of 5 wt.%, the melting enthalpies are lowered by 14.3% kJ/kg of pure paraffin wax for MWCNT nanoparticles.

Table 4.1: Comparison of MWCNT's thermal properties and conductivities with those of other composite PCMs in the literature.

Reference	**MWCNT Load (wt.%)**	**Phase Change Enthalpy (kJ/kg)**		**Thermal Conductivity (W/mk)**
		Melting	**Solidification**	**At range 10°C - 50°C**
(Li-Wu Fan et al, 2013)	0	208	205	0.260 - 0.275
	1	195	200	0.270 - 0.280
	2	193	198	0.275 - 0.320
	3	185	190	0.280 - 0.330
	4	180	180	0.290 - 0.360
	5	178	180	0.310 - 0.390
				At range 20°C - 35°C
(Vellaisamy Kumaresan et al, 2012)	0.00	136.20	114.10	0.285 - 0.140
	0.15	137.20	130.30	0.290 - 0.170
	0.30	127.28	120.40	0.360 - 0.180
	0.45	129.50	122.60	0.385 - 0.185
	0.60	133.60	120.00	0.390 – 0.200
				At range 15°C - 60°C
(Deqiu Zou et al, 2017)	0	N/A	N/A	0.38
	0.2	N/A	N/A	0.44
	0.5	N/A	N/A	0.50
	0.8	N/A	N/A	0.52
	1	N/A	N/A	0.54
	1.2	N/A	N/A	0.56
	1.5	N/A	N/A	0.58
				At range 40°C - 75°C
(TingXian Li et al, 2014)	0	200		0.25
	1.0	195		0.80
	5.0	186		0.90

(Vellaisamy Kumaresan et al, 2012) proposed the variation in thermal conductivity with respect to temperature for various Nano fluids PCMs displayed in Figure 4.1 based on data in Table 4.1. From the figure it is shown that in the solid state the thermal conductivity of all Nano fluids PCMs is higher than in the liquid state. After the beginning of solidification, thermal conductivity begins to increase and reaches its maximum value at the end of solidification. Because of the PCM's inherent poor thermal conductivity, this higher thermal conductivity of the Nano fluids PCMs near the temperature change of phase is a desirable factor for making it advantageous for any thermal storage application.

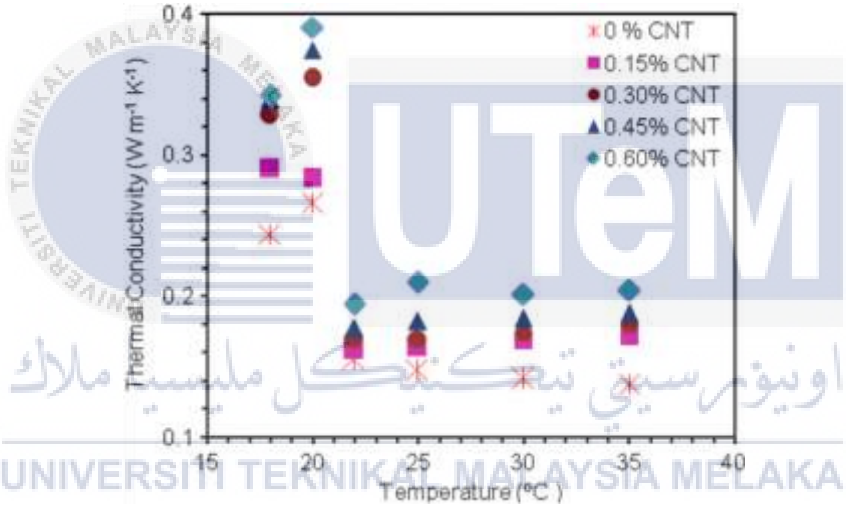

Figure 4.1: Variation in thermal conductivity for various Nano-fluid PCMs.

However, the main phase change properties of the NFPCMs at the different scanning levels of 1°C/min and 3°C/min respectively are given in the Table 4.2 and Table 4.3 proposed by (Vellaisamy Kumaresan et al, 2012). It is seen from the figures that the freezing temperature of Nano fluids PCMs varies with the MWCNT concentrations. With the addition of 0.15wt.% MWCNT, the freezing temperature tends to increase from 19.46°C to 20.05°C at 1°C/min, and 19.75°C at 3°C/min at 20.07°C. The same behavior of increase in the onset of freezing temperature is observed at both scanning rates in the Nano fluids PCMs up to 0.45 wt.%

MWCNT, which clearly indicates the nucleating action of the carbon nanotubes in the Nano fluids PCMs. In addition, the degree of super cooling of Nano fluids PCMs is reduced to a maximum of 37.44% and 35.97% at scanning rates of 1°C/min and 3°C/min with the addition of 0.15 wt.% MWCNT, respectively. The decrease in the degree of super cooling is also found in the different MWCNT concentrations of all Nano fluids PCMs. However, the effect is higher at the lower MWCNT concentration and therefore an optimal MWCNT concentration range exists, at which the degree of super cooling is minimal.

Table 4.2: Phase change in properties of the PCM and NFPCM at 1°C/min (Vellaisamy Kumaresan et al, 2012).

MWCNT (vol.%)	T_f (°C)	T_{mp} (°C)	T_{fp} (°C)	DT (°C)	DHm (Jg^{-1})	DHf (Jg^{-1})
0	19.46	20.58	18.39	2.19	136.20	114.10
0.15	20.05	20.27	18.90	1.37	137.20	130.30
0.30	21.15	20.53	18.76	1.77	127.28	120.40
0.45	21.50	20.48	18.69	1.79	129.50	122.60
0.60	20.00	20.45	18.69	1.76	133.60	120.00

Table 4.3: Phase change of the PCM and NFPCM properties at 3°C/min (Vellaisamy Kumaresan et al, 2012).

MWCNT (vol.%)	T_f (°C)	T_{mp} (°C)	T_{fp} (°C)	DT (°C)	DHm (Jg^{-1})	DHf (Jg^{-1})
0	19.75	21.30	16.63	4.67	128.90	105.10
0.15	20.07	20.67	17.68	2.99	136.60	121.30
0.30	21.52	21.07	17.32	3.75	127.70	112.70
0.45	21.75	21.06	17.24	3.82	130.50	113.40
0.60	20.48	20.93	17.25	3.68	130.20	113.60

(Deqiu Zou et al,2017) state that PCM's thermal conductivity has been measured at room temperature by the Hot Disk thermal constant analyzer. Table 4.1 shows the MWCNT-based composite PCM thermal conductivities with different added amounts of wt.%. It is observed that the addition of carbon additives will boost PCM's thermal conductivity, and the thermal conductivity increases as carbon additives increase. The higher the percentage of additives used, therefore, the higher the thermal conductivity of the PCMs.

It showed the melting processes of composite PCMs in Figure 4.2. It is shown that the transient temperature curve is obviously divisible into three phases. Phase change has not begun during the first stage and its heat transfer depends on thermal conductivity, the temperatures increase rapidly in an approximately linear fashion. As illustrated in Figure 4.2, the higher thermal conductivity of composite PCM clearly indicates a faster heating rate than that of pure paraffin.

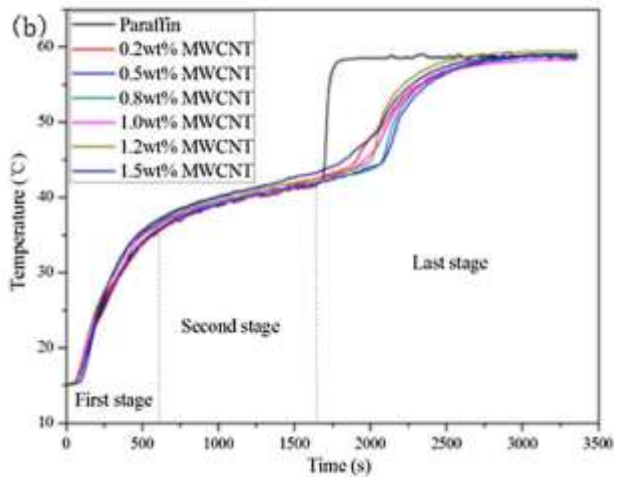

Figure 4.2: Melting curves of pure PCM and composite PCM (MWCNT as additives) (Deqiu Zou et al,2017).

During the second stage, PCMs start melting and consuming a significant amount of heat in the process of phase change, the temperatures rise at a very slow rate. PCM has completely melted during the last stage, as natural convection begins to be involved in heat transfer with the accelerated disturbance, the temperature curve slope is showing a sharp rise. This can also be easily seen that when the additive sum is raised to 1.0%, the slope is smaller.

The freezing of composite PCMs processes was shown in Figure 4.3. The transient temperature curve may also be divided into three stages, similar to the melting process. It is observed that all composite PCM with different additive contents during the entire discharge process have a higher temperature decrease rate than the pure PCM.

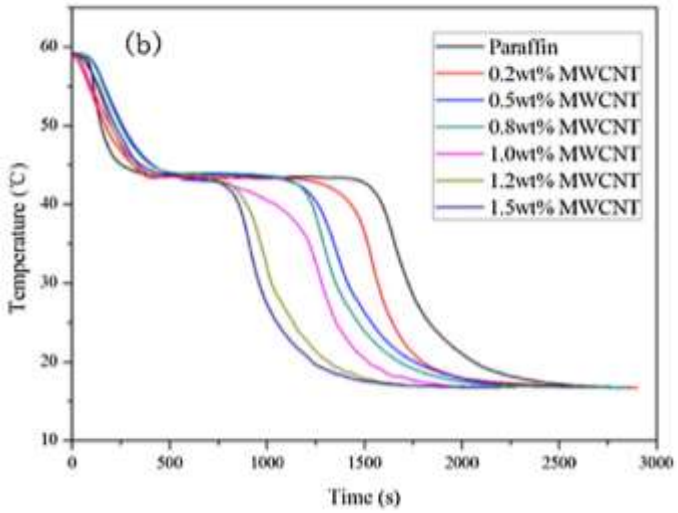

Figure 4.3: Freezing curves of pure PCM and composite PCM (MWCNT as additives) (Deqiu Zou et al,2017).

DSC analysis was used in this experiment conducted by (Murugan P et al, 2017). The DSC technique is useful in determining many of a material's thermodynamic properties, such as melting and freezing temperatures, unique heat, phase change enthalpies, etc. Figure 4.4 shows the DSC analysis of the various NPCM.The application of MWCNT in base PCM only has a slight effect on the peak temperature of the melt. However, in the case of NPCM, the onset of solidification is advanced by the MWCNT over that of the base PCM. This clearly indicates that the nucleating action of the MWCNT and the maximum advancement in the onset of solidification is present in the NPCM containing 0.6 wt.%.

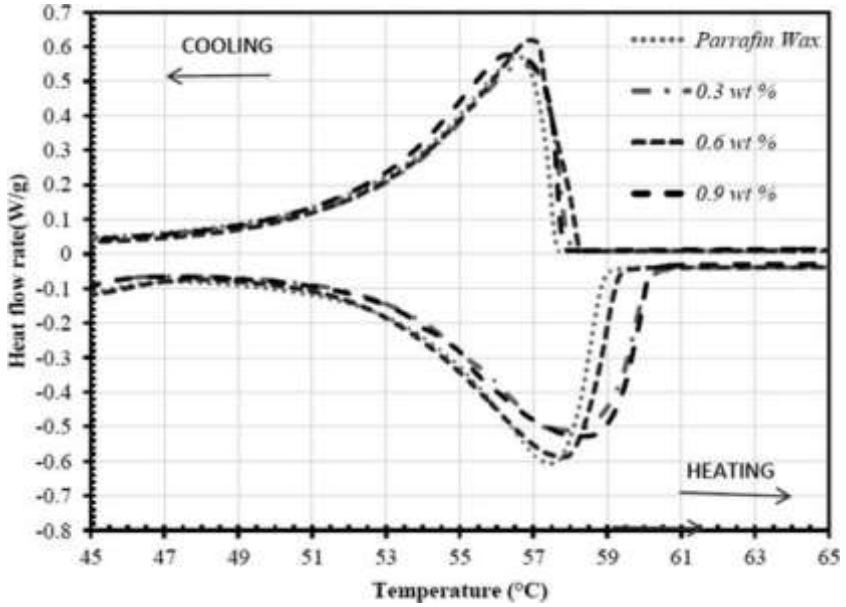

Figure 4.4: DSC analysis of the various NPCM (Murugan P et al, 2017).

Table 4.4 describes the main phase changes in properties such as the initiation of solidifying / melting and the resulting latent heat. It is well known that the total area under both extremes, during melting and solidification, reflects the corresponding latent heat of the base PCM and NPCM. It is interesting to note that NPCM's latent heat is higher than base PCM's. The latent heat of melting and solidification in the NPCM with 0.9 wt. % is enhanced to a maximum of 12.5% and 8.2% compared to that of the base PCM. The possible reason could be due to the augmentation in molecular heat transport in the base PCM with the presence of MWCNT.

Table 4.4: Major phase change properties of the base PCM and NPCM at 1°C/min (Murugan P et al, 2017).

MWCNT (wt. %)	T_m (°C)	T_f (°C)	Tmp (°C)	Tfp (°C)	DH_m (J g^{i1})	DH_f (J g^{i1})
0	47.28	57.85	57.55	56.61	131.8	139.2
0.3	47.36	58.28	58.08	56.67	137.5	135.8
0.6	48.20	58.55	57.83	56.93	147.6	140.6
0.9	46.95	58.46	58.35	56.36	148.3	150.7

4.3 Second Experiment

Next, the experiment conducted by (X. Li et al, 2017), the final selection is Gamma aluminum oxide (γ-Al_2O_3, 50nm, purity >99.9) compare to Copper, Cu to increase the thermal conductivity of the PCM. The reason why Gamma aluminum oxide (γ-Al_2O_3) was selected will be discuss in this subtopic. The main material is anhydrous calcium chloride ($CaCl_2$, purity>96%). Table 4.5 shows the Copper, Cu as a comparison of nanoparticles in terms of latent heat and thermal conductivity.

Table 4.5: Copper, Cu as nanoparticles comparison in term of latent heat and thermal conductivity.

Reference	Copper Weight Percentage (wt.%)	Latent Heat (kJ/kg)		Thermal Conductivity (W/mk.)	
		Melting (°C)	Solidification (°C)	Liquid State (60°C)	Solid State (25°C)
S. Y. Wu et al (2012)	0	-	-	0.170	0.27
	0.5	-	-	0.185	0.28
	1.0	-	-	0.188	0.29
	1.5	-	-	0.190	0.30
	2.0	-	-	0.200	0.31
S. Wu et al (2010)	0	205	202	-	-
	0.5	202	196	-	-
	1.0	197	190	-	-
	1.5	182	179	-	-
	2.0	181	178	-	-
P Zhang. et al (2017)	0	175.24		0.1	0.3
	Copper foam	380		401	
B. Xu et al (2018)	0	199.77	206.6	0.25	
	0.1	126.85	127.55	0.92	

(S. Y. Wu et al, 2012) said the storage and release rate of energy depends heavily on the thermal conductivity of PCMs. Given Cu nanoparticle's high thermal conductivity, Cu/paraffin is expected to have greater thermal conductivity than pure paraffin. Figure 4.5 illustrates the thermal conductivity values of PCMs as a function of Nano particular concentration in solid and liquid states. This shows that the thermal conductivity of the PCMs is improved nonlinearly with concentration of Cu nanoparticles. That is because Cu nanoparticles can agglomerate in paraffin liquids. The higher the concentration of Cu/paraffin, the smoother the agglomeration is

for the Cu nanoparticles. The agglomeration will then significantly reduce the amount of effective dispersed nanoparticles and thereby decrease the increase in thermal conductivity per wt.% point.

The highest thermal conductivity changes were observed in this study at up to 14.2% in solid state and 18.1% in liquid state at 2 wt.% Cu/paraffin. (SK et al, 2006), likewise, reported similar results. He showed that the increase in thermal conductivity of Cu nanoparticles in nano fluids exceeded approximately 10.7% at 0.1 wt.% volume.

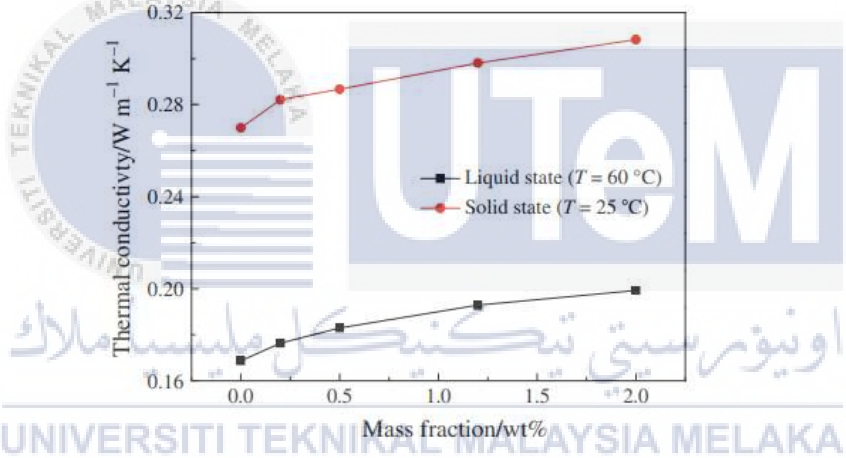

Figure 4.5: Thermal conductivity values of liquid and solid PCMs (S. Y. Wu et al,2012).

(S. Wu et al, 2010) According to the theory of mixtures, Cu/paraffin composite latent heat is equal to the values determined by multiplying the latent heat value of pure paraffin in the composite PCM with its mass fraction. The measured values are expressed in Figure 4.6. It shows that each composite's latent heat is smaller than the latent heat calculated. With the increase of Cu's mass fractions, the deviation is getting bigger.

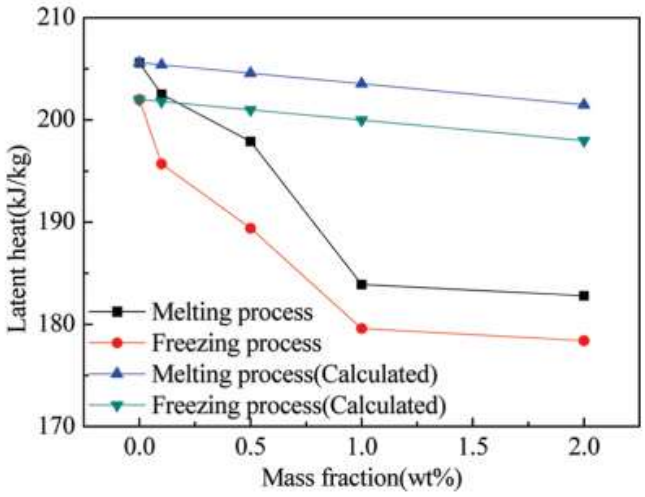

Figure 4.6: Latent heat of Cu/paraffin with different mass fractions (S. Wu et al, 2010).

(B. Xu et al, 2018) The melting and freezing temperatures for paraffin were measured at 61.17°C and 56.31°C. Of the composite the melting and freezing temperatures were estimated at 57.44°C and 54.38°C. Compared to pure paraffin, paraffin@$CuCu_2O$ composite melting and freezing temperatures apparently decreased. This may have been due to the fact that paraffin was encapsulated within a micrometric space, and its molecular motion was confined within the given geometry, resulting in a reduction in melting and freezing temperatures (K Jiang et al, 2008).

Therefore, (X. Li et al, 2017) use the Gamma aluminum oxide (γ-Al_2O_3) in the experiment. In order to investigate an effective nanoparticle of CaCl2·6H2O nanocomposite PCMs, heating-cooling experiments were conducted with nanoparticles γ-Al_2O_3, TiO_2, Cu, and SiO_2, respectively, whereas the content of all nanoparticles was set at 0.5 wt.%, as reported by X. Li et al (2017). Figure 4.7 shows the cooling curve of nanocomposite PCMs from $CaCl_2 \cdot 6H_2O$. It is obvious that the $CaCl_2 \cdot 6H_2O$ plus nucleating agent exhibits a significant super cooling degree about 5.3°C. In addition, the degree of super cooling of the $CaCl_2 \cdot 6H_2O$

nanocomposite PCMs with various nanoparticles (γ-Al_2O_3, TiO_2, Cu, and SiO_2) was 0.2, 2.2, 5.4 and 9.5°C respectively.

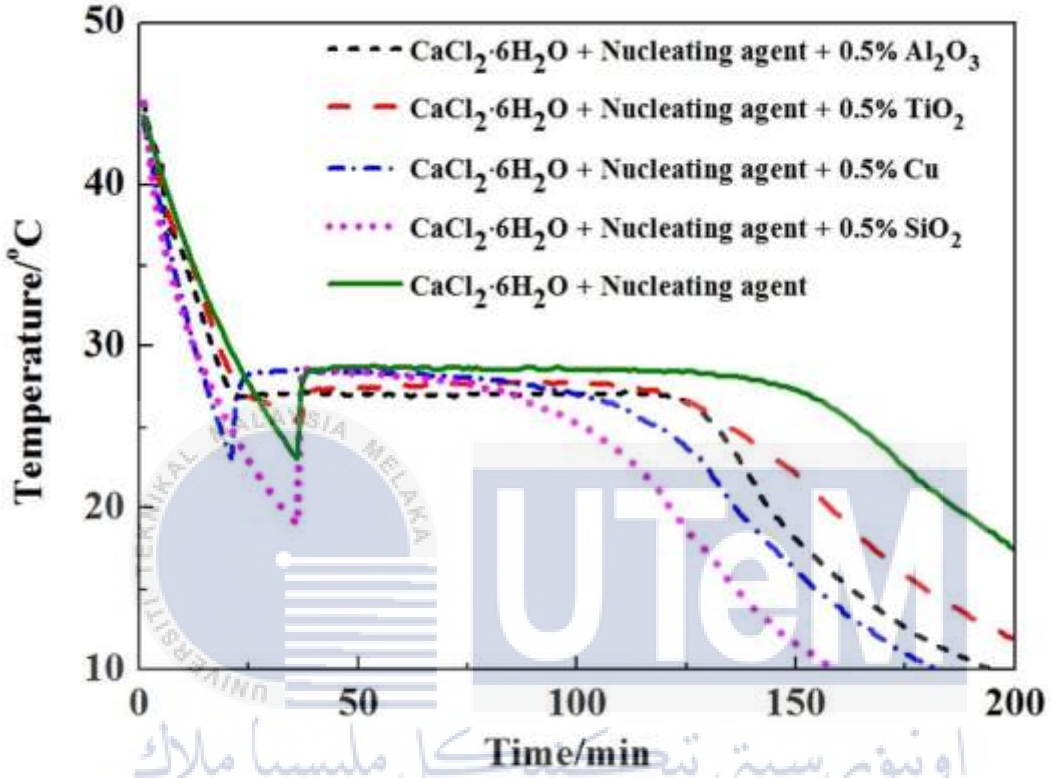

Figure 4.7: Cooling curves of the PCMs with different nanoparticles (X. Li et al, 2017).

(X. Li et al, 2017) also stated that too many hydroxyl groups on the surface of the SiO_2 and Cu nanoparticles, which have the opposite effect for the growth of $CaCl_2 \cdot 6H_2O$ in crystallization. Hence, the nanoparticles γ-Al_2O_3 have the best performance to reduce the degree of super cooling. Figure 4.8 illustrates the transmission electron microscopy (TEM) photographs of the irregularly shaped γ-Al_2O_3 nanoparticles categorized as the nucleating agent with a diameter of about 50 nm.

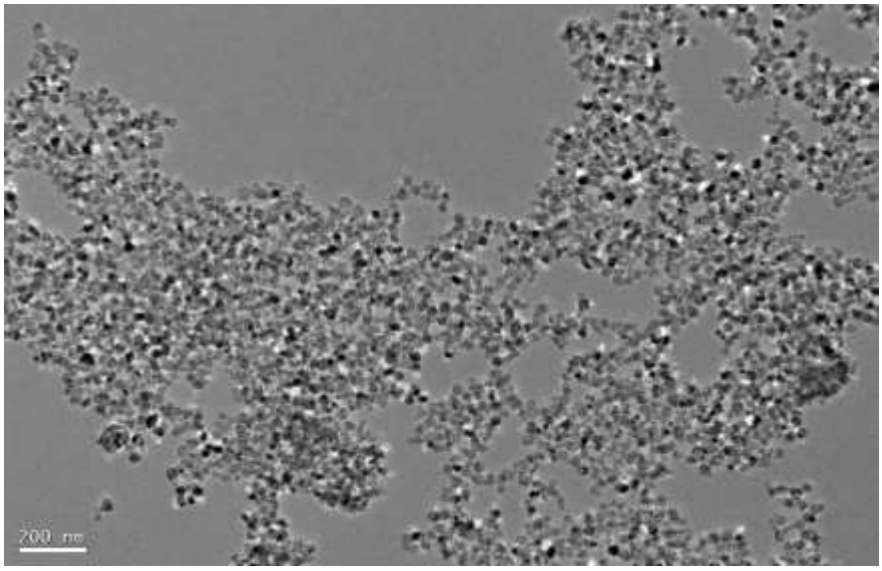

Figure 4.8: TEM photographs of γ-Al_2O_3 nanoparticles (X. Li et al, 2017).

The relationship between the concentration of γ-Al_2O_3nanoparticles and the degree of super cooling of the nanocomposite PCM is shown in Figure 4.9 based on the data in Table 4.6. To ascertain the correct values, the measurements were performed in triplicate. Figure 4.10 shows the latent heats of $CaCl_2 \cdot 6H_2O$ nanocomposite PCMs with respect to the mass fraction of nanoparticles γ-Al_2O_3.

Table 4.6: Latent Heat and Thermal Conductivity of Gamma-Aluminum Oxide (X. Li et al, 2017).

Reference	Gamma-Aluminum Oxide Weight Percentage (wt.%)	Temperature (°C)		Latent Heat (kJ/kg)		Thermal Conductivity (W/mk.)
		Freezing Process	Super cooling Degree	Theory	Experimental	
X. Li et al (2017)	0	29	5.27	179	179	0.341
	0.5	28	0.17	178	177	0.459
	1.0	28	0.23	177	174	0.672
	1.5	27	0.30	176	163	0.976
	2.0	27	0.70	175	156	1.373

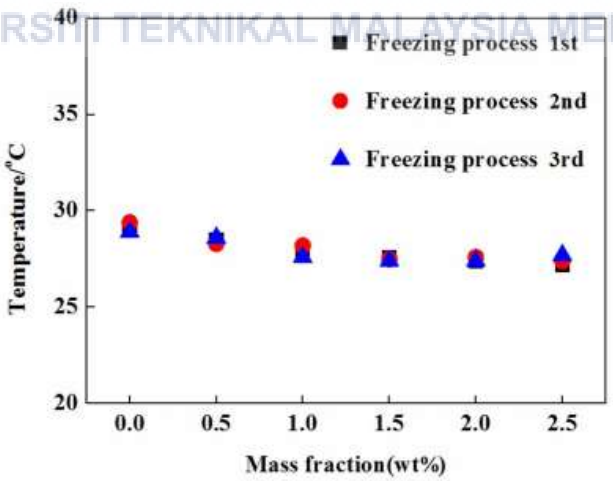

Figure 4.9: The relationship between the γ-Al2O3 nanoparticles concentration and the super cooling degree of the nanocomposite PCM (X. Li et al, 2017).

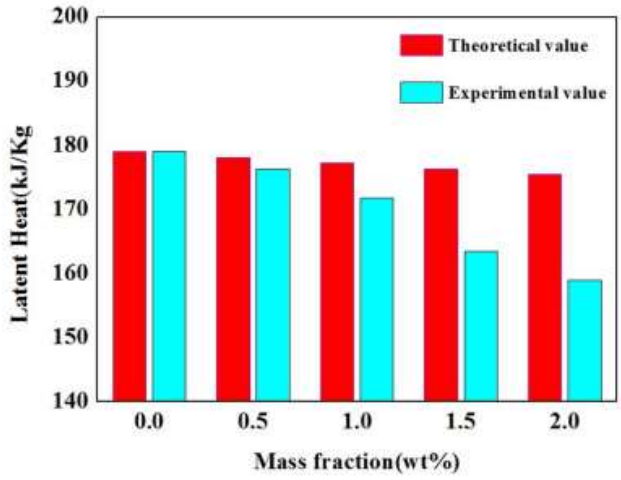

Figure 4.10: Latent heat of $CaCl_2 \cdot 6H_2O$ /γ-Al_2O_3 nanocomposite PCMs with different mass fractions (X. Li et al, 2017).

Based on Figure 4.10, the maximum reduction is 9% for latent heats of $CaCl_2 \cdot 6H_2O$ nanocomposite PCMs with different nanoparticles (0.5wt.%, 1.0wt.%, 1.5wt.%, and 2.0wt.%). The latent heat of the $CaCl_2 \cdot 6H_2O$ nanocomposite PCMs is equal, according to the theory of mixtures, to the values calculated following the multiplication of the latent heat value of $CaCl_2 \cdot 6H_2O$ with its mass fraction in the composite PCM. The calculated values are shown in Figure 4.10 which indicates that each composite's latent heat was lower than the latent heat calculated. Given that the heat transfer performance of the nanocomposite PCMs is different from that of the conventional solid-liquid mixture, the increase in the nanoparticles mass fractions resulted in greater deviations.

The thermal conductivity of the $CaCl_2 \cdot 6H_2O$ nanocomposite PCMs with 0.5wt.%, 1.0wt.%, 1.5wt.%, and 2.0wt.% nanoparticles showed a marked increase following an increase in the amount of nanoparticles presented in Figure 4.11 based on data in Table 4.6 in the composite as shown. The conductivity of the CaCl2·6H2O PCM was 0.341 W/mK. The conductivities of the $CaCl_2 \cdot 6H_2O$ / γ-Al_2O_3 (0.5, 1.0, 1.5, and 2.0 wt.%) nanocomposite PCMs

were 0.459 W/m·K, 0.672 W/m·K, 0.976 W/m·K and 1.373 W/m·K, increased by 34.6%, 97%, 186% and 303%, respectively, which is indicative of the primary contribution of γ-Al_2O_3 nanoparticles in obtaining a high thermal conductivity. The addition of γ-Al_2O_3 nanoparticles was not only beneficial in reducing the degree of super cooling, but also facilitated thermal conductivity improvement. In addition, thermal conductivity improvements also impacted heat storage and heat release times.

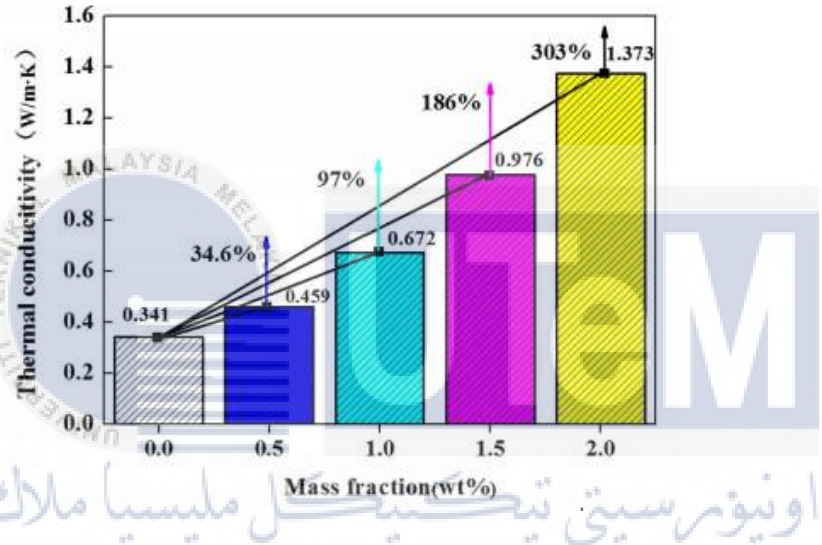

Figure 4.11: Thermal conductivity of $CaCl_2 \cdot 6H_2O$ / γ-Al_2O_3 nanocomposite PCMs

Table 4.7 presents the measurement results and standard deviation of super cooling degree of the nanocomposite PCM. The results indicate that the super cooling degree of the $CaCl_2 \cdot 6H_2O$ /γ-Al_2O_3 nanocomposite PCMs was within the range of 0–2°C, which is indicative of the additional latent heat released by the nanocomposite PCMs. Therefore, we can conclude that $CaCl_2 \cdot 6H_2O$ /γ-Al_2O_3 nanocomposite PCMs has better thermal conductivity compare to other nanocomposite PCMs (TiO_2, Cu, and SiO_2).

Table 4.7: The measurement results and standard deviation of super cooling degree of the nanocomposite PCM (X. Li et al, 2017).

Samples	Super cooling degree /°C			Average/°C	Standard Error
	1st	2nd	3rd		
$CaCl_2 \cdot 6H_2O$	5.3	4.9	5.6	5.27	0.350
0.5%γ-Al_2O_3-$CaCl_2 \cdot 6H_2O$	0.2	0.1	0.2	0.17	0.058
1.0%γ-Al_2O_3-$CaCl_2 \cdot 6H_2O$	0.3	0.2	0.2	0.23	0.058
1.5%γ-Al_2O_3-$CaCl_2 \cdot 6H_2O$	0.4	0.2	0.3	0.30	0.100
2.0%γ-Al_2O_3-$CaCl_2 \cdot 6H_2O$	0.8	0.6	0.7	0.70	0.100
2.5%γ-Al_2O_3-$CaCl_2 \cdot 6H_2O$	1.1	1.2	1.3	1.20	0.100

Figure 4.12 illustrates the heat storage and heat release curves of the $CaCl_2 \cdot 6H_2O$/γ-Al_2O_3 nanocomposite PCMs, with a $CaCl_2 \cdot 6H_2O$ equilibrium temperature increase from 15°C to 40°C after 75 minutes in the heat storage curve. The temperature was also showing a slow rise with a relatively long heat storage platform at temperature 27°C – 29°C. The addition of the nanoparticles 0.5, 1.0, 1.5, and 2.0 wt.% γ-Al_2O_3 showed a rise in temperature from 15°C to 40°C after 68, 64, 42 and 38 min respectively. In addition, the $CaCl_2 \cdot 6H_2O$/γ-Al_2O_3 nanocomposites PCMs' full melting times were reduced by 19.33%, 14.66%, 44%, and 49.33%, respectively, suggesting an increased composite heat transfer efficiency. The heat release curves

indicate that the temperature of $CaCl_2 \cdot 6H_2O$ dropped from 40°C to 15°C after 454 min, while the nanocomposite PCMs of $CaCl_2 \cdot 6H_2O/\gamma\text{-}Al_2O_3$ showed the same temperature drop within only 339 min – 410 min. The complete solidification times of $CaCl_2 \cdot 6H_2O/\gamma\text{-}Al_2O_3$ nanocomposites PCMs have been reduced by 9.69%, 17.84%, 19.38%, and 25.33%. After melting and freezing a large amount of heat is absorbed and discharged, respectively. Consequently, by adding the nanoparticles, the thermal conductivity of PCMs was increased. In terms of its macroscopic properties, the heat storage and release times required to obtain the temperature of the equilibrium were reduced in the nanocomposite PCMs of $CaCl_2 \cdot 6H_2O/\gamma\text{-}Al_2O_3$. Additionally, heat release takes so much longer than the process of storing heat. Under the same conditions the melting rate is faster than the solidification rate. It is presented as the heat release takes so much longer than the heat storage process macroscopically.

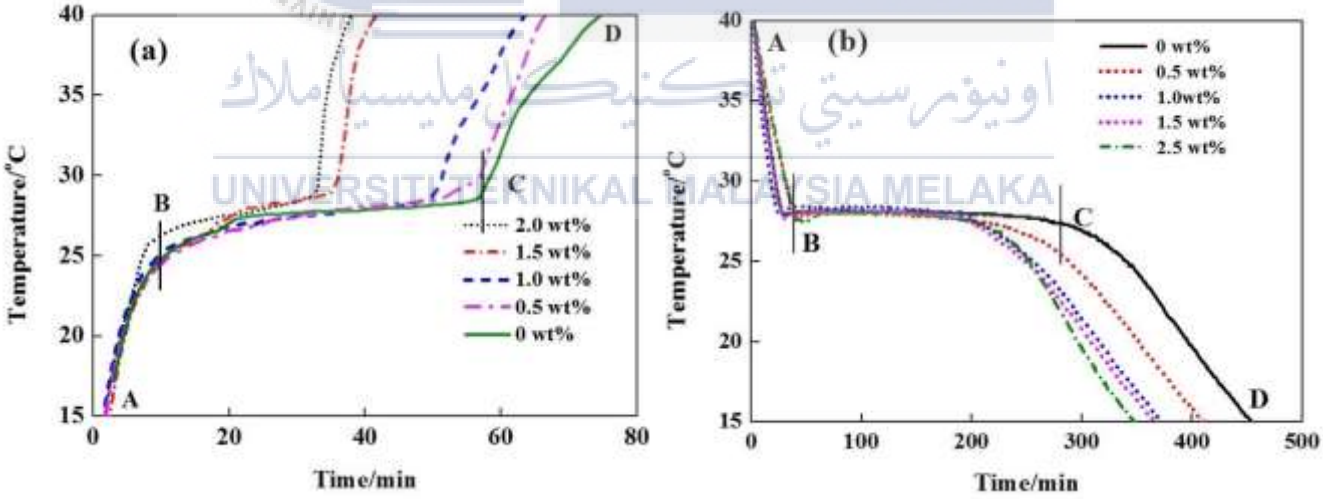

Figure 4.12: (a) Heat storage curves and (b) Heat release curves of $CaCl_2 \cdot 6H_2O/\gamma\text{-}Al_2O_3$ nanocomposite PCMs with different mass fractions.

Although thermal cyclic operations are inherent in long-term melting and solidification operations, it is essential for PCMs to minimize or eliminate any undesirable phase change temperature and latent heat changes during the melting and solidification of composite PCMs as these changes affect energy storage and release rates. The $CaCl_2 \cdot 6H_2O$ nanocomposite PCMs with 1.0 wt.% γ-Al_2O_3 nanoparticles as tested for ascertaining the long-term thermal stability.

4.4 Third Experiment

Last but not least, the experiment conducted by (F. Cheng et al ,2017), the pure PCM is used with graphite expanded to increase the PCM's thermal conductivity. Paraffin (Tm = 58°C-60°C) was used as PCMs in composite PCM preparation.

4.4.1 Enhanced Thermal Conductivity due to Various Graphene Nano fillers Comparison of the Data among Available Literature

The effects of the size and thickness of graphene Nano fillers on their performance are therefore of great importance, having shown that GNPs have better performance in serving as thermal conductivity fillers because of their low thermal interface resistance caused by geometry. Because of the availability in the present work it was unable to compare directly between different GNPs with different sizes and thicknesses. A comparison between the findings presented and the evidence published in the literature available, i.e. Refs. [(Kim S. et al, 2009), (Yavari F. et al, 2011), (Xiang JL. et al, 2011), (Shi J-N et al, 2013), (Chen Y-J et al, 2013)]. Therefore, in relation to thermal conductivity enhancement of graphene-based nanocomposite PCMs, an effort is made to reveal the size effects of graphene Nano fillers on their performance. Although the graphene Nano fillers adopted in these studies were synthesized following the similar thermal exfoliation protocol as described in Table 4.8, the sizes and shapes

of the resulting graphene products spread across a wide range due to specific conditions applied for chemical intercalation, thermal expansion, and mechanical exfoliation. Comparison of measured data on relative enhancement between these relevant studies is shown in Figure 4.13, where the legendary abbreviations can be referenced in Table 4.8. It is noted that the present data were collected at 10°C, and at room temperature the data from the available literature were measured. Due to the great uncertainties associated with the size, thickness and dispersion of the various graphene Nano fillers, which complicates the external comparison between references, significant discrepancy is seen for the data reported by different researchers.

Table 4.8: Descriptions of the different graphene Nano fillers adopted in the literature available for preparation of nanocomposite PCMs.

References	Materials	Synthesis methods	Dimensions		Loadings
			Sizes	Thickness	
(Kim S. et al, 2009)	xGnP[a]	Thermal exfoliation of intercalated graphite	15 lm	<10 nm	Up to 7 wt.%
(Yavari F. et al, 2011)	Graphene	Thermal exfoliation of intercalated graphite	N/A	3–4 layers	Up to 4 wt.%
(Xiang JL. et al, 2011)	xGnP-1[b] xGnP-15	Thermal exfoliation of intercalated graphite	15 lm 1 lm	10 nm	up to 10 wt.%
(Shi J-N et al, 2013)	Graphene xGnP	Thermal exfoliation of intercalated graphite	N/A	N/A	Up to 10 wt.%
(Chen Y-J et al, 2013)	R-GN[c] O-GN	Thermal exfoliation of intercalated graphite	N/A	30–100 nm	Up to 5 wt.%

[a] xGnP stands for exfoliated graphite Nano platelets.

[b] xGnP-1 and xGnP-15 stand for xGnP with an average size of 1 and 15 lm, respectively.

[c] R-GN and O-GN stand for graphite Nano sheets with random and oriented distributions, respectively

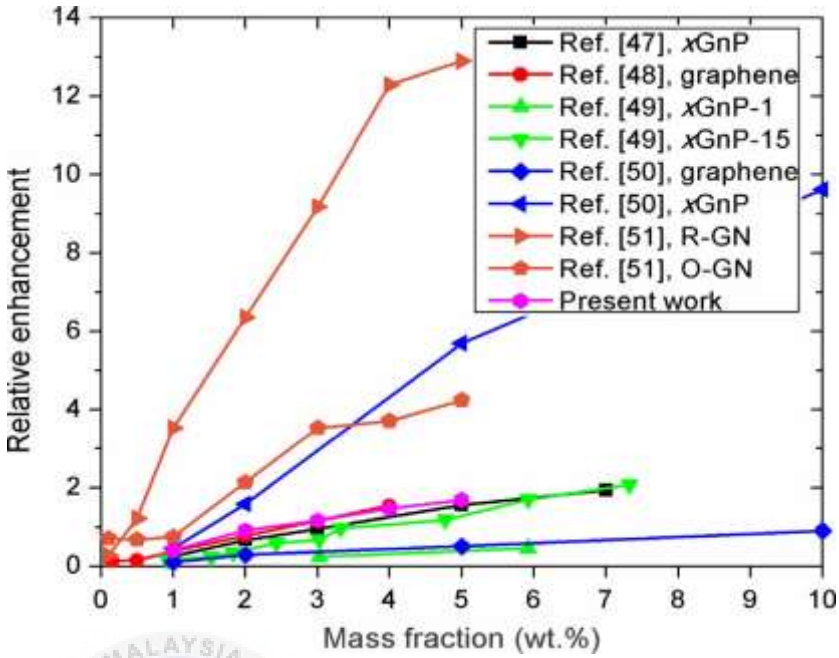

Figure 4.13: Comparison of the relative thermal conductivity improvement of nanocomposite PCMs due to the existence of different Nano fillers of graphene.

Although the alleged graphene Nano fillers sizes and thicknesses vary significantly, the present data are in good agreement with those reported by (Yavari F. et al, 2011) and are in fairly good agreement with those reported by (Kim S. et al, 2009) and (Xiang JL. et al, 2011) with the 15-lm xGnP. However, the bundle of these four curves represents only moderate thermal conductivity enhancement. The enhancement reported by (Chen Y-J et al, 2013) is significantly greater than the others, and they found that random distribution of the fillers is preferred due to better heat transfer networks being formed.

Furthermore, for the two studies where a clear internal comparison was possible, a consensus was reached that reducing the size and thickness of graphene Nano fillers is undesirable because the larger and thicker graphene Nano fillers, i.e. xGnP-15 in Reference of (Xiang JL. et al, 2011) and xGnP in Reference of (Shi J-N et al, 2013), resulted in much greater thermal conductivity enhancements. This is likely due to increased thermal interface resistance due to increased phonon on scattering at the smaller graphene Nano fillers interfaces.

4.4.2 Detail Comparison from Literature Review.

The pure PCM is used with extended graphite to improve the thermal conductivity of the PCM for the third experiment performed by (F. Cheng et al ,2017) Paraffin (Tm = 58°C – 60°C) was used as PCMs to render composite PCMs. Table 4.9 below shows the thermal conductivity and similarities of the previous researcher's utilization of graphene/graphite particles.

Table 4.9: Graphene/Graphite as nanoparticles comparison in term of latent heat and thermal conductivity.

Reference	Graphene/Graphite Weight Percentage (wt.%)	Melting Temperature (°C)	Total Latent Heat Capacity (kJ/kg)	Thermal Conductivity (W/mk.)
(Ahmet Sari et al, 2007)	0	41.6	194.6	0.220
	2	41.1	192.6	0.399
	4	41.0	188.0	0.520
	7	40.7	181.9	0.680
	10 (form-stable PCM)	40.2	178.3	0.820
(Deqiu Zou et al, 2018)	0	N/A	N/A	0.38
	0.2	N/A	N/A	0.46
	0.5	N/A	N/A	0.54
	0.8	N/A	N/A	0.62
	1.0	N/A	N/A	0.66
	1.2	N/A	N/A	0.70
	1.5	N/A	N/A	0.76

(Ahmet Sari et al, 2007) Figure 4.14 shows thermal conductivity of composite PCMs with different mass fractions of EG, suggesting that the thermal conductivity increased with an increased mass fraction of EG. From Figure 4.15 it is easy to draw a relationship between the thermal conductivity and the mass fraction of the EG:

$$\hat{y} = 0.0524_x + 0.3038 \, (r^2 = 0.9974) \quad (2)$$

Where $\hat{y}$ *and* x represent thermal conductivity (k) and mass fraction of EG (%), respectively. The high determination coefficient (r^2 = 0.9974) suggested a close link between the thermal conductivity and the EG mass fraction.

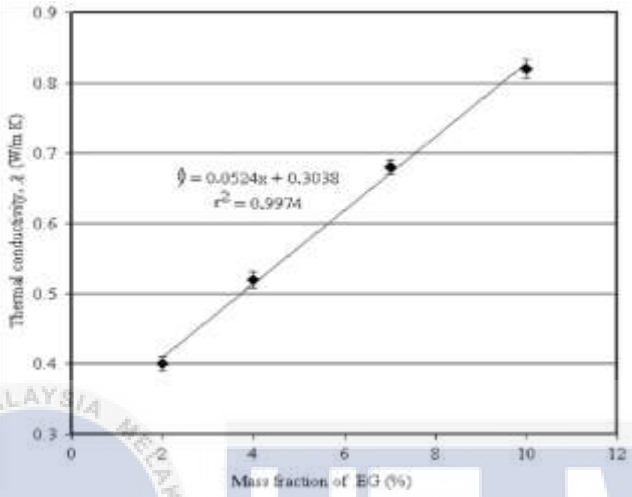

Figure 4.14: Thermal conductivities of paraffin/EG composite PCMs with varying mass fraction of EG (Ahmet Sari et al, 2007).

The thermal conductivity of the composite PCMs with a mass fraction of 2%, 4%, 7% and 10% EG indicated that paraffin thermal conductivity (0.22 W/mK) increased as 81.2%, 136.3%, 209.1% and 272.7% respectively. This was because of the EG's high thermal conductivity. The results also showed that more than 10 wt.% could further achieve the thermal conductivity of paraffin by adding EG. However, this mass fraction is sufficient to obtain form-stable composite PCM, and further increase in EG by more than 10 wt.% would result in a decrease in the composite 's latent heat capacity due to a decrease in the composite's mass fraction of paraffin (less than 90 wt.%). The mass fraction of EG in the composite was therefore reduced by 10%. In passive LHTES applications, the high thermal conductivity of form-stable composite PCM (about four times that of pure paraffin) makes this much more desirable than pure paraffin.

(Deqiu Zou et al, 2018) Figure 4.15 shows the melting processes of the composite PCMs. It is shown that the transient temperature curve is obviously divisible into three phases. Phase change has not started during the first stage and its heat transfer depends on thermal conductivity, the temperatures rise rapidly in an approximately linear manner. The composite PCM with higher thermal conductivity clearly shows a faster heating rate than that of pure paraffin, as shown in Figure 4.16. In addition, with the increase in addition amount, the temperature rise rate was increased while the extent for graphene based composite PCM was greater. For example, for pure paraffin the time for temperature to rise from 15 C to 35 C is 600 s. For graphene-based composite PCM, the period is 495 s, 490 s, 400 s, 390 s, 385 s, and 380 s respectively when the added quantities are 0.2%, 0.5%, 0.8%, 1.0%, 1.2% and 1.5% respectively.

At the second stage, PCMs start melting and consuming a significant amount of heat in the process of phase change, the temperatures rise at a very slow rate. PCM has completely melted during the last stage, as natural convection starts to be involved in heat transfer with the accelerated disturbance, the temperature curve slope is showing a sharp rise. It can also be clearly found that when the additive amount is increased to 1.0%, the slope becomes smaller.

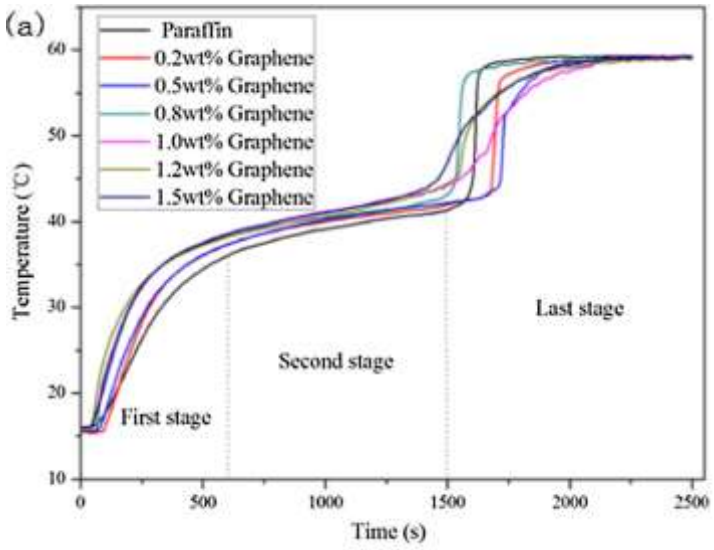

Figure 4.15: Melting curves of pure PCM and composite PCM (graphene as additives) (Deqiu Zou et al, 2018).

The freezing of composite PCMs processes was shown in Figure 4.16. The transient temperature curve may also be divided into three stages, similar to the melting process. It is observed that all composite PCM with different additive contents during the entire discharge process have a higher temperature decrease rate than the pure PCM, and the magnitude for graphene-based composite PCMs has been greater. For example, the time for pure paraffin to decrease temperature from 60°C to 20°C is 2060 s. For graphene-based composite PCM, the time is 1750s, 1650s, 1350s, 1230s, 1170s, and 1120s, respectively, when the added amounts are 0.2%, 0.5%, 0.8%, 1.0%, 1.2%, and 1.5%.

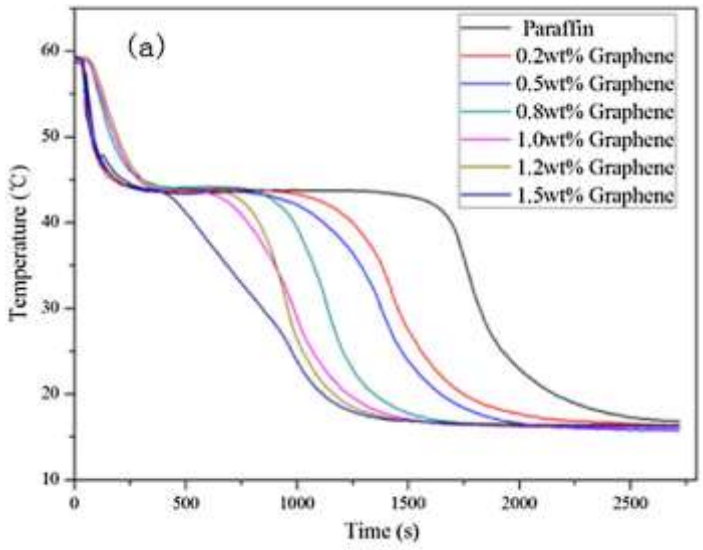

Figure 4.16: Freezing curves of pure PCM and composite PCM (graphene as additives) (Deqiu Zou et al, 2018).

The thermal properties and conductivities of EG / paraffin composites from literature with comparable PCMs are described in Table 4.10. It can be realized that the prepared EG / paraffin composite shows a relatively high thermal enthalpy, a proper temperature and thermal conductivity for a building energy storage system. Thus, the EG / paraffin exhibits adequate power for thermal energy storage systems.

Table 4.10: The literature compared the thermal properties and conductivities of prepared composite PCM with that of other composite PCMs (F. Cheng et al, 2017).

Reference	Composite PCM	Melting point (°C)	Latent heat (J/g)	Freezing point (°C)	Latent heat (J/g)	Thermal conductivity [W/(m K)]
(A. Karaipekli et al, 2009)	Paraffin/expanded vermiculite	48	110	52.5	113.1	0.545
(C. Li et al, 2013)	Paraffin/expanded perlite	42.27	87.40	40.79	90.25	0.046
(Z.Y. Yin et al, 2016)	Paraffin/carbon foam	44.51	105.8	48.48	105.8	-
(Fei Cheng et al, 2017)	EG/paraffin composite	44.95	126.4	47.05	125.6	3.13
	LWM of 20 wt.% EG/paraffin composite	46.52	23.82	43.74	23.36	0.76

4.4.3 Analysis Method

For this research conducted by (F. Cheng et al, 2017), the FT-IR analysis and XRD analysis were used to collect the data for determining the thermal conductivity. The FT-IR spectra of the paraffin, EG, EG/paraffin composites and the samples with different content of EG/paraffin composites are gathered in Figure 4.17 (F. Cheng et al, 2017). On the other hand, the absorption peaks on the EG/paraffin composites curve include almost all the typical absorption peaks observed for both EG and paraffin without revealing any new peaks of

absorption. It can therefore be concluded that there was no chemical interaction between EG and paraffin. In other words, the paraffin is essentially preserved by capillary and surface tension forces in the EG pores, stopping the molten paraffin from escaping from the composites. Figure 4.17(b) shows that samples with added EG / paraffin composites have identical absorption peaks as the EG / paraffin composites, and the peak amplitude increases with the added EG / paraffin composite numbers.

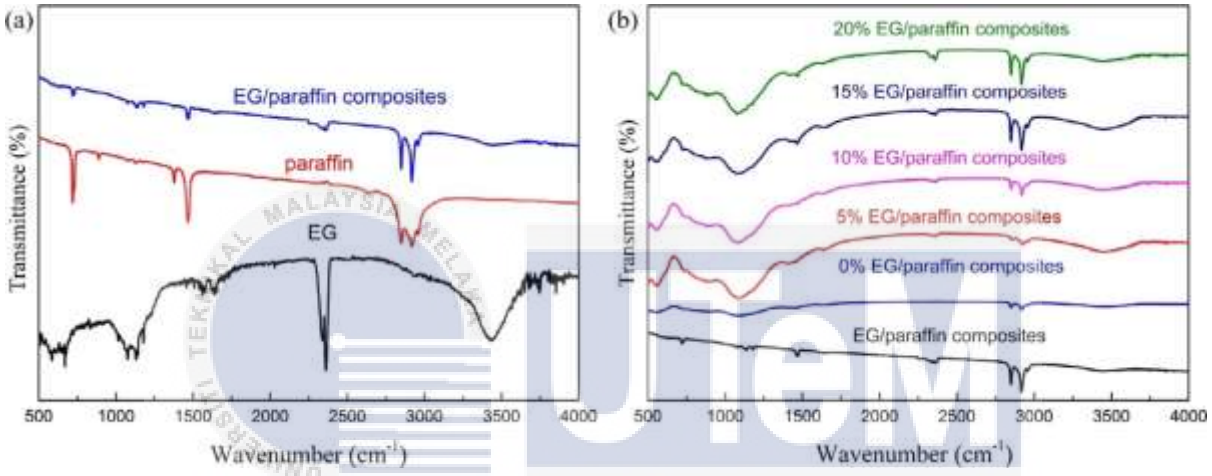

Figure 4.17: (a) FT-IR spectrum of EG, paraffin and EG/paraffin composites; (b) FT-IR spectrum of EG/paraffin composites and the groups from S1 to S5 (F. Cheng et al, 2017).

Figure 4.18(a) depicts the characteristic XRD patterns for paraffin, EG, and EG/paraffin composites (F. Cheng et al, 2017). The peak at 26.5 in EG is attributable to their regular crystal structure. The paraffin XRD curve contains two major peaks, at 21.4 and 23.7. On the other hand, the EG/paraffin composites XRD pattern consists of both the EG and paraffin patterns. That suggests that the EG and paraffin crystal structure remained unchanged. Figure 4.18(b) shows the XRD patterns of EG / paraffin composites and LWMs with the addition of 0% and 15% content of EG/paraffin composites. It should be noted that the sample with a content of 15% includes the characteristic peaks of EG/paraffin composite and no peaks of EG/paraffin

were found in the sample with 0%. This shows that there was no chemical reaction between the composites EG/paraffin and fly ash.

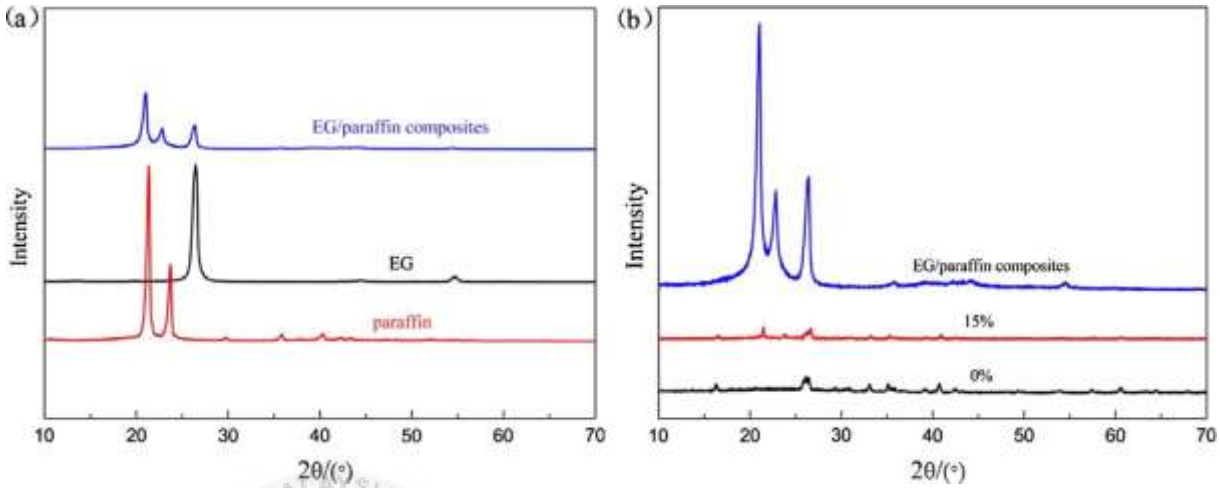

Figure 4.18: (a) XRD patterns of EG, paraffin, and EG/paraffin composites; (b) XRD patterns of EG/paraffin composites and the LWMs with 0% and 15% content of EG/paraffin composites added into (F. Cheng et al, 2017)

The thermal conductivity may be calculated after the data have been obtained by using this two analysis. The most important thermal conductivity parameter for the PCM is. (F. Cheng et al, 2017) Paraffin with low thermal conductivity can increase the response time for latent heat melting and freezing, as stated above. Therefore, an important parameter in material design processes is improving thermal conductivity. Because of the high thermal conductivity of EG (2.90 W/mK) (Wu S. et al, 2009), the introduction of EG could increase the thermal conductivity of the composites. The EG was thus selected to increase the conductivity of the PCM composites.

Figure 4.19 illustrates the sample thermal conductivity from S1 from S5, and the calculated thermal conductivity is given in Table 4.11. Pure paraffin will be noted to be in solid state (20°C). Table 4.11 shows that the thermal conductivity of the solid state sample group S1

was measured as 0.39 W/mK, and the values for S2, S3, S4 and S5 were 0.43, 0.49, 0.69 and 0.76 W/mK respectively. These findings suggest that if compared to the content of 0%, the thermal conductivity of the wall material containing EG/paraffin composite was subsequently increased. It can be concluded that EG/paraffin composite exhibited higher thermal conductivity, and hence becomes a preferred PCM for wall material.

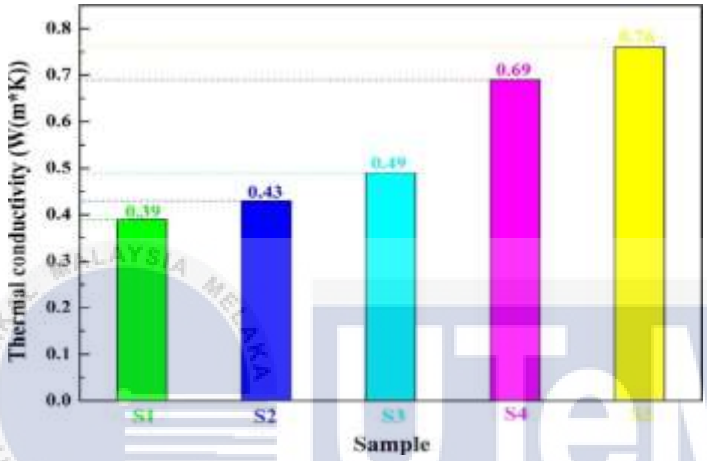

Figure 4.19: Thermal conductivities of the sample from S1 from S5 (F. Cheng et al, 2017).

Table 4.11: Thermal conductivities of the groups S1–S5 (F. Cheng et al, 2017).

Experiment group	Content of EG/paraffin composites (%)	a 10^6 (m^2/s)	q 10^3 (kg/m^3)	Cp 10^3 [J/(kg K)]	k [W(m K)]
S1	0	0.288	0.401	3.31	0.39
S2	5	0.309	0.429	3.21	0.43
S3	10	0.362	0.438	3.09	0.49
S4	15	0.514	0.452	2.98	0.69
S5	20	0.573	0.471	2.82	0.76

CHAPTER 5

CONCLUSION AND RECOMMENDATION

This chapter summarizes general conclusions that can be drawn from the results of this project and suggests areas where additional research or refinement is needed.

5.1 Conclusion

In a nutshell, the addition of nanoparticles significantly increased the transfer of heat from PCMs in phase change. After researching MWCNT-based, copper-based and graphene-based composite PCM respectively, composite PCM was prepared and characterized with varying proportions of MWCNT, copper and graphene to make the PCM suitable for a storage device. A new phase change material which is called "advanced nanocomposite" $CaCl_2 \cdot 6H_2O$ / γ-Al_2O_3 nanocomposite PCMs was prepared and the action of phase change was systematically studied. The following can be summarized for achieving the results:

1) Nanoparticles with high thermal conductivity have shown tremendous potential in heat transfer applications because of their small size and particular thermal properties. Zeng et al. added Cu nanoparticles and multi-walled carbon nanotubes (MWNTs) to improve the thermal conductivity of PCMs. Ho et al, studied the thermophysical properties of emulsion from nanoparticles in paraffin (n-octadecane) prepared by emulsifying nanoparticles from Al_2O_3. Those authors concluded that with the weight percentage wt.% of γ-Al_2O_3 nanoparticles, the thermal conductivity of Al_2O_3/paraffin increased the highest compare to other nanocomposites. Therefore, the "advanced nanocomposite" $CaCl_2 \cdot 6H_2O$ / γ-Al_2O_3 is

selected as the best material used to enhance the phase change material thermo-physical properties.

2) It is interesting to note that NPCM's latent heat is higher than base PCM's. Based on research conducted by (Murugan P et al, 2017), the latent heat of melting and solidification in the NPCM with 0.9 wt. % is enhanced to a maximum of 12.5% and 8.2% compared to that of the base PCM. The possible reason could be due to the augmentation in molecular heat transport in the base PCM with the presence of MWCNT. Therefore, the higher the weight percentage wt.% of nanoparticles, will result in decreasing of the latent heat of PCMs, thus increase and enhance the thermal conductivity, k value of thermal energy storage (TES).

Implementing nanofluids and PCMs may be good for performance on the system. These materials will however introduce a new set of complications that need to be addressed. Several important questions must be tackled to solve the prominent issues in this field, which are listed below:

1. What is the optimum weight percentage, wt.% of nanomaterial in base fluid and PCM, to produce a nanofluid/nano-PCM that balances between thermal conductivity enhancement and corresponding cost?
2. How, during the mixing process, to avoid agglomeration and sedimentation of nanoparticles, to produce ideal nanofluids?
3. How many cycles of heating-cooling can PCM and nanoPCM endure without degradation?

An interesting way to satisfy these criteria is to combine nano-PCM and nanofluids. Finding the right maintenance mechanism, however, remains a bit of an issue.

5.2 Recommendation for Future Works

In the area of thermal energy storage, further work is required using phase change materials. Following are recommendations for future research:

- Studying the thermal cycling stability of PCM when performing sufficient freezing/melting cycles and under the conditions of actual operation.
- Investigation of thermal losses after thermal storage for a period of time in case of thermal energy storage using phase change materials and compare it with energy storage using pure paraffin.
- To research the long-term stability of the TCM composites produced based on $CaCl_2 \cdot 6H_2O$ / γ-Al_2O_3, which display promising results.
- Investigation of new materials which have a high thermal conductivity to be used for thermal energy storage as phase-change materials.

REFERENCES

[1] Ali, M. A., Fayaz, Viegas, R. F., Shyam Kumar, M. B., Kannapiran, R. K., & Feroskhan, M. (2019). Enhancement of heat transfer in paraffin wax PCM using nano graphene composite for industrial helmets. *Journal of Energy Storage*, *26*(October), 100982. https://doi.org/10.1016/j.est.2019.100982

[2] Byung Chul Shin, Sang Done Kim, & Won-Hoon, P. (1989). Phase separation and Super cooling of a latent heat-storage material. *Energy*, *14*(12), 921–930. https://doi.org/10.1016/0360-5442(89)90047-9

[3] Chang, T. C., Lee, S., Fuh, Y. K., Peng, Y. C., & Lin, Z. Y. (2017). PCM based heat sinks of paraffin/nanoplatelet graphite composite for thermal management of IGBT. *Applied Thermal Engineering*, *112*, 1129–1136. https://doi.org/10.1016/j.applthermaleng.2016.11.010

[4] Cheng, F., Wen, R., Huang, Z., Fang, M., Liu, Y., Wu, X., & Min, X. (2017). Preparation and analysis of lightweight wall material with expanded graphite (EG)/paraffin composites for solar energy storage. *Applied Thermal Engineering*, *120*, 107–114. https://doi.org/10.1016/j.applthermaleng.2017.03.129

[5] Cheng, W. L., Zhang, R. M., Xie, K., Liu, N., & Wang, J. (2010). Heat conduction enhanced shape-stabilized paraffin/HDPE composite PCMs by graphite addition: Preparation and thermal properties. *Solar Energy Materials and Solar Cells*, *94*(10), 1636–1642. https://doi.org/10.1016/j.solmat.2010.05.020

[6] De Gracia, A., & Cabeza, L. F. (2015). Phase change materials and thermal energy storage for buildings. *Energy and Buildings*, *103*, 414–419. https://doi.org/10.1016/j.enbuild.2015.06.007

[7] Dincer, I. (2002). On thermal energy storage systems and applications in buildings. *Energy and Buildings*, *34*(4), 377–388. https://doi.org/10.1016/S0378-7788(01)00126-8

[8] Kahwaji, S., Johnson, M. B., Kheirabadi, A. C., Groulx, D., & White, M. A. (2018). A comprehensive study of properties of paraffin phase change materials for solar thermal energy storage and thermal management applications. *Energy*, *162*, 1169–1182. https://doi.org/10.1016/j.energy.2018.08.068

[9] Khanafer, K., Vafai, K., & Lightstone, M. (2003). Buoyancy-driven heat transfer enhancement in a two-dimensional enclosure utilizing nanofluids. *International Journal of Heat and Mass Transfer*, *46*(19), 3639–3653. https://doi.org/10.1016/S0017-9310(03)00156-X

[10] Kibria, M. A., Anisur, M. R., Mahfuz, M. H., Saidur, R., & Metselaar, I. H. S. C. (2015). A review on thermophysical properties of nanoparticle dispersed phase change materials. *Energy Conversion and Management*, *95*, 69–89. https://doi.org/10.1016/j.enconman.2015.02.028

[11] Li, X., Zhou, Y., Nian, H., Zhang, X., Dong, O., Ren, X., … Shen, Y. (2017). Advanced Nanocomposite Phase Change Material Based on Calcium Chloride Hexahydrate with Aluminum Oxide Nanoparticles for Thermal Energy Storage. *Energy and Fuels*, *31*(6), 6560–6567. https://doi.org/10.1021/acs.energyfuels.7b00851

[12] Manca, O., Jaluria, Y., & Poulikakos, D. (2010). Heat transfer in nanofluids. *Advances in Mechanical Engineering*, *2010*. https://doi.org/10.1155/2010/380826

[13] Mantilla Gilart, P., Yedra Martínez, Á., González Barriuso, M., & Manteca Martínez, C. (2012). Development of PCM/carbon-based composite materials. *Solar Energy Materials and Solar Cells*, *107*, 205–211. https://doi.org/10.1016/j.solmat.2012.06.014

[14] Mohamad, A. T., & Che Sidik, N. A. (2019). Nano-enhanced phase change material effects on the Super cooling degree improvement: A review. *IOP Conference Series: Materials Science and Engineering*, *469*(1). https://doi.org/10.1088/1757-899X/469/1/012036

[15] Murugan, P., Ganesh Kumar, P., Kumaresan, V., Meikandan, M., Malar Mohan, K., & Velraj, R. (2018). Thermal energy storage behaviour of nanoparticle enhanced PCM during freezing and melting. *Phase Transitions*, *91*(3), 254–270. https://doi.org/10.1080/01411594.2017.1372760

[16] Qu, Y., Wang, S., Zhou, D., & Tian, Y. (2020). Experimental study on thermal conductivity of paraffin-based shape-stabilized phase change material with hybrid carbon nano-additives. *Renewable Energy*, *146*, 2637–2645. https://doi.org/10.1016/j.renene.2019.08.098

[17] Shanthi, R., Anandan, S. S., & Ramalingam, V. (2012). Heat transfer enhancement using nanofluids an overview. *Thermal Science*, *16*(2), 423–444. https://doi.org/10.2298/TSCI110201003S

[18] Sidik, N. A. C., Kean, T. H., Chow, H. K., Rajaandra, A., Rahman, S., & Kaur, J. (2018). Performance enhancement of cold thermal energy storage system using nanofluid phase change materials: A review. *International Communications in Heat and Mass Transfer*, *94*(1), 85–95. https://doi.org/10.1016/j.icheatmasstransfer.2018.03.024

[19] Wong, K. V., & De Leon, O. (2010). Applications of nanofluids: Current and future. *Advances in Mechanical Engineering, 2010*. https://doi.org/10.1155/2010/519659

[20] Wu, S., Zhu, D., Li, X., Li, H., & Lei, J. (2009). Thermal energy storage behavior of Al2O3-H2O nanofluids. *Thermochimica Acta*, *483*(1–2), 73–77. https://doi.org/10.1016/j.tca.2008.11.006

[21] Xuan, Y., & Li, Q. (2000). Heat transfer enhancement of nanofluids. *International Journal of Heat and Fluid Flow*, *21*(1), 58–64. https://doi.org/10.1016/S0142-727X(99)00067-3

[22] Zalba, B., Marín, J. M., Cabeza, L. F., & Mehling, H. (2003). Review on thermal energy storage with phase change: Materials, heat transfer analysis and applications. In *Applied Thermal Engineering* (Vol. 23). https://doi.org/10.1016/S1359-4311(02)00192-8

[23] Zhang, Z., & Fang, X. (2006). Study on paraffin/expanded graphite composite phase change thermal energy storage material. *Energy Conversion and Management*, *47*(3), 303–310. https://doi.org/10.1016/j.enconman.2005.03.004

[24] Zheng, H., Wang, C., Liu, Q., Tian, Z., & Fan, X. (2018). Thermal performance of copper foam/paraffin composite phase change material. *Energy Conversion and Management*, *157*(September 2017), 372–381. https://doi.org/10.1016/j.enconman.2017.12.023

[25] Li-Wu F, Xin F, Xiao W, et al. Effects of various carbon nanofillers on the thermal conductivity and energy storage properties of paraffin-based nanocomposite phase change materials. Appl Energy. 2013;110:163–172.

[26] Vellaisamy K, Ramalingam V, Sarit KD. The effect of carbon nanotubes in enhancing the thermal transport properties of PCM during solidification. Heat and Mass Transfer. 2013;48:1345–1355.</bib>

[27] Xiang Li, Zhou, Y., Nian, H., Zhang, X., Dong, O., Ren, X., … Shen, Y. (2017). Advanced Nanocomposite Phase Change Material Based on Calcium Chloride Hexahydrate with Aluminum Oxide Nanoparticles for Thermal Energy Storage. *Energy and Fuels*, *31*(6), 6560–6567. https://doi.org/10.1021/acs.energyfuels.7b00851

[28] Sarı, A., Alkan, C., Karaipekli, A., & Uzun, O. (2009). Microencapsulated n-octacosane as phase change material for thermal energy storage. Solar Energy, 83(10), 1757–1763. doi: 10.1016/j.solener.2009.05.008

[29] Wu SY, Wang H, Xiao S, et al. An investigation of melting/freezing characteristics of nanoparticle-enhanced phase change materials. J Therm Anal Calorim. 2012;110:1127–1131.

[30] Das SK. Nanofluids—the cooling medium of the future. Heat Transfer Eng. 2006;27(10)

[31] Shuying W, Dongsheng Z, Xiurong Z. Preparation and melting/freezing characteristics of Cu/paraffin nano-fluid as phase change material (PCM). Energy Fuel. 2010;24:1894–1898.

[32] A. Karaipekli, A. Sarı, K. Kaygusuz, Thermal characteristics of paraffin/expanded perlite composite for latent heat thermal energy storage, Energy Sourc. Part A: Recov. Util. Environ. Eff. 31 (10) (2009) 814–823.

[33] C. Li, H. Yang, Expanded vermiculite/paraffin composite as a solar thermal energy storage material, J. Am. Ceram. Soc. 96 (2013) 2793–2798.

[34] Z.Y. Yin, Z.H. Huang, R.L. Wen, X.G. Zhang, B. Tan, Y.G. Liu, X.W. Wu, M.H. Fang, Preparation and thermal properties of phase change materials based on paraffin with expanded graphite and carbon foams prepared from sucroses, RSC ADV. 6 (2016) 95085.

[35] Fei Cheng, Ruilong Wen, Zhaohui Huang *, Minghao Fang, Yan'gai Liu, Xiaowen Wu, Xin Min, Preparation and analysis of lightweight wall material with expanded graphite (EG)/paraffin composites for solar energy storage. Applied Thermal Engineering 120 (2017) 107-114

[36] Cheng, F., Wen, R., Huang, Z., Fang, M., Liu, Y., Wu, X., & Min, X. (2017). Preparation and analysis of lightweight wall material with expanded graphite (EG)/paraffin composites for solar energy storage. Applied Thermal Engineering, 120, 107–114. https://doi.org/10.1016/j.applthermaleng.2017.03.129

[37] Kim S, Drzal LT. High latent heat storage and high conductive phase change materials using exfoliated graphite nanoplatelets. Sol Energy Mater Sol Cells 2009;93:136–42

[38] Yavari F, Fard HR, Pashayi K, Rafiee MA, Zamiri A, Yu Z, et al. Enhanced thermal conductivity in a nanostructured phase change composite due to low concentration graphene additives. J Phys Chem C 2011; 15:8753–8.

[39] Xiang JL, Drzal LT. Investigation of exfoliated graphite nanoplatelets (xGNP) in improving thermal conductivity of paraffin wax-based phase change material. Sol Energy Mater Sol Cells 2011; 95:1811–8.

[40] Shi J-N, Ger M-D, Liu Y-M, Fan Y-C, Wen N-T, Lin C-K, et al. Improving the thermal conductivity and shape-stabilization of phase change materials using nanographite additives. Carbon 2013; 51:365–72.

[41] Li-Wu Fan, Xin Fang, Xiao Wang et al. Effects of various carbon nanofillers on the thermal conductivity and energy storage properties of paraffin-based nanocomposite phase change materials. Applied Energy 110 (2013) 163-172.

[42] TingXian Li, Ju-Hyuk Lee, RuZhu Wang, Yong Tae Kang. Heat transfer characteristics of phase change nanocomposite materials for thermal energy storage application. International Journal of Heat and Mass Transfer 75 (2014) 1-11.

[43] Drissi, S., Eddhahak, A., Caré, S., & Neji, J. (2015). Thermal analysis by DSC of Phase Change Materials, study of the damage effect. Journal of Building Engineering, 1, 13–19. doi: 10.1016/j.jobe.2015.01.001

[44] Kajita, S., Yoshida, N., Yoshihara, R., Ohno, N., Yokochi, T., Tokitani, M., & Takamura, S. (2012). TEM analysis of high temperature annealed W nanostructure surfaces. Journal of Nuclear Materials, 421(1-3), 22–27. doi: 10.1016/j.jnucmat.2011.11.044

[45] Karaipekli, A., & Sarı, A. (2009). Capric–myristic acid/vermiculite composite as form-stable phase change material for thermal energy storage. Solar Energy, 83(3), 323–332. doi: 10.1016/j.solener.2008.08.012

[46] Deqiu Zou, Xianfeng Ma, Xiaoshi Liu, Pengjun Zheng, Yunping Hu. Thermal performance enhancement of composite phase change materials (PCM) using graphene and carbon nanotubes as additives for the potential application in lithium-ion power battery. International of Journal Heat & Mass Transfer 120 (2018) 33-